A MODEL-REFERENCE SLIDING MODE CONTROL FOR DUAL-STAGE ACTUATOR IN HARD DISK DRIVE

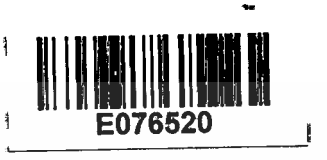

SIWAPHON SONKHAM

A THESIS SUBMITTED IN PARTIAL FULFILLMENT
OF THE REQUIREMENT FOR THE DEGREE OF
MASTER OF ENGINEERING IN DATA STORAGE TECHNOLOGY
INTERNATIONAL COLLEGE
KING MONGKUT'S INSTITUTE OF TECHNOLOGY LADKRABANG
2013

KMITL-2013-IC-M-005-009

Thesis	A Model-Reference Sliding Mode Control for Dual-Stage Actuator in Hard Disk Drive
Student	Mr. Siwaphon Sonkham
Student ID.	52600628
Degree	Master of Engineering (M.E.)
Program	Data Storage Technology
Year	2013
Thesis Advisor	Asst. Prof. Dr. Unnat Pinsopon
Thesis Co-Advisor	Assoc. Prof. Dr. Withit Chatlatanagulchai

ABSTRACT

This thesis presents a method of sliding mode control (SMC) designing and developing for the servo system in a dual-stage actuator (DSA) hard disk drive. The mathematical modeling of the hard disk drive actuators was obtained by extracting from the measuring frequency response of the voice-coil motor (VCM) and the PZT micro-actuator separately. The Matlab software tools were used for mathematical model estimation and also for the controller design and simulation. A model-reference approach for the tracking requirements has been selected as a proposed technique in this study. The time-domain simulation results showed that the performances of a model-reference SMC controller in DSA servo system could be satisfied in the tracking error under the presence of internal and external disturbance in track-following mode. It shows the ability to keep the head position within the boundary of +/-10% of track width. The performances of the proposed model-reference SMC controlled DSA system met all requirement specifications. The reduction of the positioning error (PES) was significantly obtained when compared to the single-state actuator (SSA). The performances of the proposed controller design were also compared to the conventional PID control. The results showed that the model-reference SMC design could overcome the classical PID technique for the tracking performance benchmarking.

Acknowledgements

I would like to extend my sincere gratitude to my advisor Asst. Prof. Dr. Unnat Pinsopon and my co-advisor Assoc. Prof. Dr. Withit Chatlatanagulchai in advising me for this research work. During the entire period of time their dedication in giving valuable advices and significant comments are highly appreciated. I would like to appreciate the thesis committees for their precious time and advices to give an admirable shape to this thesis.

Thanks are also due to my company "Western Digital Thailand" for the great moral support and also for having faith in me to complete in this research as well as a financial supporting. At the same time, I would like to thank my boss, Mr. Witthaya Keopuang for his kindness and the HSA test team of Western Digital Thailand for support during the period of study. Thanks all my colleagues who supported to the tools in helping me for my research.

Finally, I wish to thank my family, my beloved wife and my kids for all their supported and encouraged me all the time during my study the Master Degree in Data Storage Technology.

SIWAPHON SONKHAM

Content

List of Tables

List of Figures

Chapter 1
Introduction

The first Hard Disk Drive (HDD) was invented in the 1950s by a group of researchers and engineers in IBM. The first HDD is the "IBM 305" RAMAC (random access method of accounting and control). It had a capacity of about 5 MB (Mega-bytes), stored on fifty of 24-inch disks. It had bit density of 2000 bits per square inch. The first generation of HDDs used in personal computers in the early 1980s had a capacity of 10 MB. In modern HDDs, rotating disks coated with a thin magnetic layer or recording medium are written with data that are arranged in concentric circles so called "*tracks*". A disk drive stores data as magnetic patterns on one or more disks. The data bit stored as a binary represented by a polarity of each bit is detected (read) or set (written) by a read/write (R/W) head. This is done by sweeping the R/W head over the disk(s). The conventional HDD component is illustrated in Fig. 1.1. The tracks and the data bits on a disk surface should be written as closed as possible so that the usage of the disk surface could be maximized. By doing this, the increasing of track density and bit density could be achieved. The track density means the number of tracks encircling the disk in one inch radial, and the bit density means the number of bits in each track.

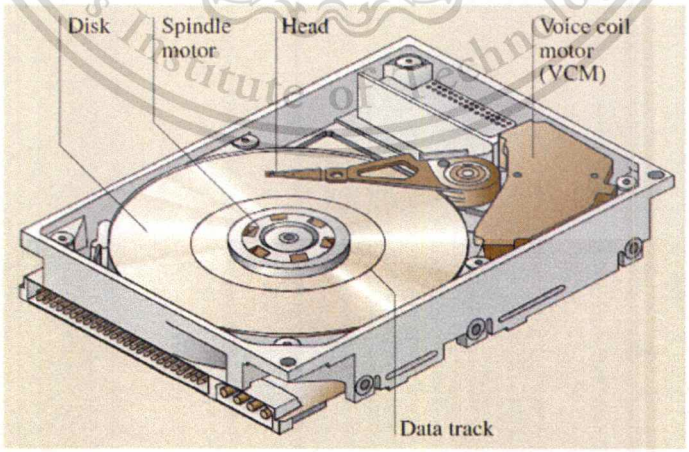

Fig. 1.1: Schematic diagram of a hard disk drive (HDD) [5].

In HDD, a media disk is the principal component that enables the storage of binary data information. The data information bits are stored in concentric data tracks on a rotating disks coated with magnetic media while the R/W head is recorded and retrieved the data information from media. A motor so called spindle-motor has a job of spinning the disk(s). An actuator arm has a function to position the R/W head accessing the desired target track. Fig.1.2 shows the important components found in a typical HDD. The actuator arm so called "*Head Stack Assembly (HSA)*" consists of a voice coil motor (VCM), an E-block arm, suspensions, and slider heads. The R/W head is fabricated on the edge of each slider (one for each disk surface). Each slider is supported by a suspension and flies over the surface of a disk on an air bearing. The VCM actuates the suspensions and sliders about a pivot in the center of the E-block.

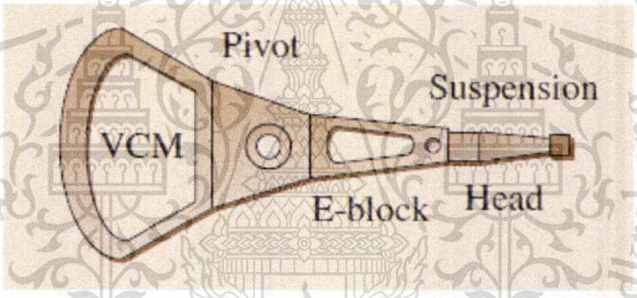

Fig. 1.2: Schematic diagram of a head stack assembly (HSA) [5].

The other major function in HDD is called "servo control system". The job of a disk drive's servo control is to position the R/W head over the bits to be read or written as they spin on the disk. However, the servo bandwidth of a traditional single-stage actuator (SSA) system is limited by the multiple mechanical resonance modes of the pivot, the E-block, the VCM and the suspension. Nonlinear friction of the pivot bearing also limits achievable servo precision.

The Dual-Stage Actuator (DSA) has been introduced as a solution to overcome the limitation. The DSA has been developed and involved by integrating piezoelectric materials mounted on a large conventional VCM to act as a secondary actuator so called "micro-actuator" as illustrated in Fig.1.3. Normally, the micro-actuator uses PZT (Lead-Zirconate-Titanate) material by utilizing the piezoelectric effects to convert from

electrical voltage to mechanical displacement. The suspension-based micro-actuator approach which the PZT actuator are placed onto the suspension of a head-gimbal assembly (HGA) at the location between the R/W head and the E-block arm, will be used in this study.

Researches in the HDD industry at the present time set the target of an areal density at 1 Tera-bits per square inch with requires track density of 500 k (kilo) tracks per inch (TPI). This implies that the track width has to be smaller than 50 nm (nanometer). This is leading to decreasing in error of the positioning of the R/W head that flies on the center of the target track during read and/or write data. The key to increase HDD servo precision is to increase the servo control bandwidth. Thus, it is necessary to introduce more advanced control techniques to achieve tighter regulation in the control of the HDD servomechanism.

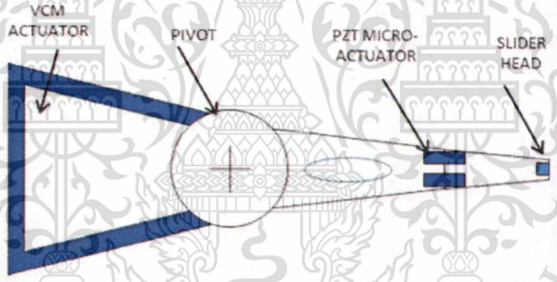

Fig. 1.3: Schematic diagram of a Dual-stage actuator in HDD.

1.1 Statement and Significance of the Problem

In HDD industry, capacity and access performances are the keys of product specifications. To achieve larger capacity, an increasing of areal density is most important, meaning that both track density and bit density are the major targets to be improved. A servo control system is the one of most several factors that need to be improved to achieve the tighter principle requirements such as a positioning accuracy in the order of a few nanometers. The implementation of the servo controller relies on the position error signal (PES), which is obtained by reading the position information encoded on the disk's data tracks. The position error is also called track mis-registration (TMR) induced from many sources of disturbances such as spindle motor run out, disk

fluttering, bias force, vibrations, shock disturbance, arm and suspension vibrations due to air turbulence, PES noise and etc. Various control design architectures and methodologies have been developed and designed for the DSA servo control. A simple rule of thumb for servo design in HDDs is that three times the statistical standard deviation (3σ) of the position error between the head and the center of the data track should be less than 1/10 of the track width (+/-10% off track). Thus, to achieve a storage density enhancement, nanometer-level precision of the servo system is required.

There are many control designs that have been developed for the DSA servo control and can be largely classified into two categories. The first group is based on the decoupled or sequential single-input single-output (SISO) designs. The other group is based on the modern optimal design methodologies such as linear quadratic Gaussian (LQG), loop-transfer recovery (LTR), H2/H∞ and etc. In existing literatures, either adaptive or robust control or both are designed to handle the disturbances and model uncertainties. Many researchers are interesting of benchmarking problem with new approach using the linear and/or nonlinear control techniques to solve the problem.

This thesis presents the design of the Sliding Mode Control (SMC) for the DSA track-following control in HDD. The SMC has been studied and proven that it has attributed to robustness for dealing with the parametric uncertainties and disturbances. The principle of the SMC method can be found from [22]-[24] and references therein. The SMC used in this study is based on a model-reference approach, suitable for tracking of the multi-input-multi-output (MIMO) systems so it could be adapted for the track-following servo control for the DSA system in HDD.

1.2 Objectives

This thesis is to develop and design a track-following DSA servo controller in order that the R/W head displacement tracks a reference input under the presence of TMR disturbances. This study will come up an alternative controller design technique for the DSA servo system in HDD. The objectives of this study are in following:

1.2.1 To obtain system identification of the DSA by extracting from its measuring data.

1.2.2 To design the SMC based on a model-reference approach for the DSA track-following servo control in HDD.

1.2.3 The performances of the proposed design has to meet the following specifications:

1.2.3.1 The mean of the steady-state error is zero.

1.2.3.2 The 3σ PES is to be less than 10% of track width under the presence of TMR disturbances.

1.2.3.3 The 5% settling time of step response is to be short as short as possible and the overshoot/undershoot is to be less than 5%.

1.2.3.4 The PZT must settle down to zero in the steady state for the next move.

1.3 Scope of the thesis

The Matlab software tools are used to obtain math model and also for controller design. The study results are to be done by simulation. The scope of this work is in the following workflow:

1.3.1 The modeling DSA used for this study is obtained using actual measurement of a 1TB HDD. The frequency response data of the DSA are measured in drive level.

1.3.2 The Matlab software tools are used to obtain and validate the mathematical model.

1.3.3 The Matlab software tools are used for controller design and simulation.

1.3.4 The TMR disturbances used for validating the controller performance is obtained from the actual measurement in disk drive operating.

1.3.5 The results of proposed technique are compared to the desired specifications.

1.3.6 The results of proposed DSA technique are compared to the SSA.

1.3.7 The results of proposed technique are compared to the conventional technique using PID (proportional integral derivative) control design.

1.4 Hypothesis

An increasing of track density results in a small track width in a few tens nanometer. The track-following servo control must be designed to be robust against the TMR disturbances. The SMC control theory has been proven that it is robustness for dealing with parametric uncertainties and disturbances. Therefore, the SMC when adapted for DSA track-following servo system in HDD should be able to accurately position the R/W head on a center track, hence achieving the growth of areal density.

1.5 Limitations and Conceptual Framework

A model-reference approach for tracking requirement has been selected as a proposed technique in this study. The performances of proposed controller design are to be evaluated. Although the DSA plant is derived from the measurement data of the actual HDD, it is not feasible to implement the proposed technique into the actual HDD for experiment at the present time. However, it is highly confident that the proposed control technique could be applied to HDD since the mathematical models have been validated and the actual measured TMR sources are used in the simulation.

1.6 Thesis Outline

The organization of this thesis is followed by:

Chapter 1 discusses about the introduction of the thesis. Basic knowledge of an HDD and components using in modern HDD are presented. The problem statement, the objective, scope of thesis and the limitation of this thesis are also discussed.

Chapter 2 presents the literatures reviewed. This could give more understanding in the background and overall of the servo control in HDD. The method of models estimation and the controller schemes for the DSA are also reviewed. The several of design methods and the problem of the TMR disturbances are also discussed in this section.

Chapter 3 introduces the mathematic modeling of the DSA using in this study. The frequency response data are measured from the actual plants. The model estimation of the DSA is extracted from its measuring data using the tools in Matlab. The

predetermined mathematical models are also validated. The theoretical principle of the SMC is also explained in this section. A model-reference SMC is designed for the DSA track-following servo control. The control parameters are determined to achieve the performance specifications.

Chapter 4 discusses the simulation results in time-domain. The 3σ PES tracking error performances of the controller design are evaluated using the measured TMR, while the settling-time and the overshoot are obtained from the step response. The performances of the proposed technique a model-reference SMC in the DSA system is compared to the SSA system, as well as benchmarking with the conventional PID control.

Chapter 5 concludes and summarizes the outcome of this work.

Chapter 2
Literature Review

There are many works that have been done recently to improve the performance of the HDD. Some of them have been studied and involved the increasing of the area density in the HDD. In this section discusses about literature reviews which could attain the fundamental knowledge of the thesis study. This section is emphasized on the reviewing of a DSA servo control in the HDD. In [1], a proposed of an idea in HDD technology development is discussed and showed that many issues could be solved by advanced controls. The suggestions are helpful for both industry and academy forums to take up challenging new innovative ideas and future works about advance techniques in the HDD servo control. The work in this section is organized as: The mathematic modeling of the HDD actuators are discussed in section 2.1. The principle of HDD servo control, key performances and design schemes are presented in section 2.2. Then the previous works based on the modern control and the decouple method are reviewed in section 2.3.

2.1 Mathematic Modeling of Actuators

2.1.1 Measurement of Frequency Response

In general, the physical HDD actuator can be represented by its frequency response and its corresponding mathematical model. In order to achieve a certain desirable performance for a given plant, it is necessary to derive an accurate model for the plant that is suitable for controller design. A typical plant model of HDD servo system includes a driver (power amplifier) and filter.

Laser Doppler Vibrometer (LDV) is a non-contact optical instrument used for accurately measuring velocity and displacement of vibrating structures. It is used to obtain the frequency response data of HDD actuator whose displacement or velocity is to be measured. The experiment measuring is repeated several times to compensate for the measurement variances. The velocity of the moving reflector can be measured by

measuring the change in frequency between the incident and the reflected beams. The LDV measures the velocity. The velocity signal is integrated to get the displacement. The measured magnitude response is in the unit of meter per volt (m/V). The schematic drawing of the experimental set-up in order to measure frequency response of an actuator in HDD is shown in Fig. 2.1 [3]. The previous study suggests that the amplitude of the swept sine used in the modeling process taken should be taken care as follows. At low frequency, the amplitude should be kept small to keep the actuator moving within acceptable range of the LDV. At higher frequency, the response of the actuator is attenuated and the input amplitude is increased to get a better measurement of gain and phase [2]-[4], [6]-[7].

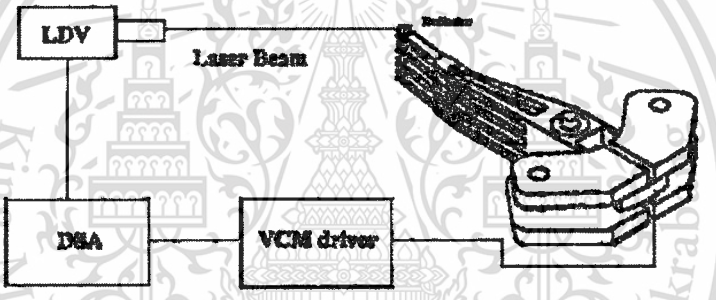

Fig. 2.1: Experimental set-up for measurement of frequency response [3].

2.1.2 Measurement of Frequency Response of Dual-Stage Actuator

Many literatures described the classical system identification techniques for the DSA in HDD. Normally, the DSA consists of a VCM and PZT micro-actuator. The VCM acts as the coarse actuator and the PZT micro-actuator gives small displacement range for improving the tracking performance of the servo control. For application in the head-positioning servomechanism of HDD, the PZT micro-actuator is fabricated as an integrated part of the suspension. The displacement of the R/W head is the combined effect of both the VCM and PZT micro-actuator as shown in Fig.2.2. The DSA is designed as a dual-input single-output (DISO) system. In the published literatures, this gives an advantage of independent measuring each of actuator separately. The experiments are carried out to get the frequency response data for each input of the DSA. The response

of the VCM is measured when the voltage of PZT micro-actuator is set to zero during this stage of measurement to ensure that the secondary actuator is not excited. Then the response of the PZT micro-actuator is measured while the VCM actuator is biased with a suitable constant current to overcome the effect of bias force exerted on the VCM actuator [6]-[10].

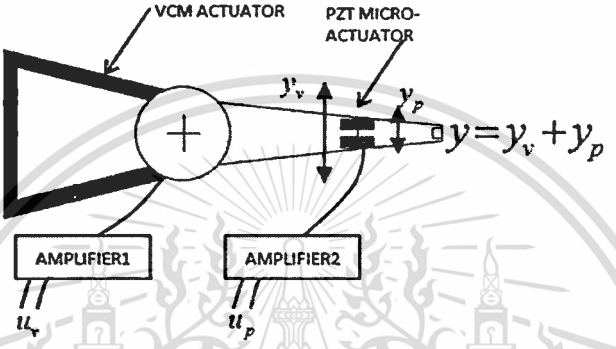

Fig. 2.2: Dual-Stage Actuator Head Position.

The alternative method for obtaining the data is simply to do it in the disk drive level by using the position measurement from the feedback control system. This method has the advantages as the extracted data are measured exactly from the system and all effects are included. Normally, this method could be done on production drives in the factory [10].

2.1.3 Identification of Transfer Function Model

The excitation signals are fed into to each of actuator driver separately and then the gain and phase response at each of the frequencies are considered. The actual dynamics model of actuators is more complex because of their resonance modes. It may need a transfer function of higher order for an accurately model. The input–output behavior of a dynamics system can be modeled using a transfer function as

$$G(s) = \frac{Y(s)}{U(s)} = \frac{B(s)}{A(s)}$$

where $Y_{(s)}$ and $U_{(s)}$ are the Laplace Transform of the output $y_{(t)}$ and input $u_{(t)}$, respectively. The transfer function, $G_{(s)}$ is the ratio of two polynomials of Laplace Transform parameter s. The frequency response data included multiple resonance modes were used to identify the transfer function of both actuators according to a Linear Time-Invariant (LTI) dynamic system. The frequency response data can be formed as.

$$\frac{B_{(S)}}{A_{(S)}} = \frac{b_0 s^m + b_1 s^{m-1} + \ldots + b_m}{a_0 s^n + a_1 s^{n-1} + \ldots + a_n}$$

Many literatures presented least-square method for model fitting on the complex plane. The principle of least-square is to minimize the sum of square of residual errors. A transfer function model is extracted from the measurement at a discrete set of frequencies. The order of the transfer function model was selected through the cost functions obtained from least-square estimation (LSE) technique for different orders of the transfer function.

$$LSE = \sum_{k=1}^{n} \left| \frac{Aj\omega_k}{Bj\omega_k} - Gj\omega_k \right|^2$$

The frequency response of a linear dynamic system represents its input–output behavior in the steady state that can be expressed by two parameters – *Gain* (K) and *Phase* (θ) representing the amount of attenuation or magnification and phase-shift, respectively. The effectiveness of the proposed technique has been verified in modelling of a hard disk drive actuator [3]-[6], [9]-[10].

The example plot of the frequency response model of the VCM actuator and the PZT micro-actuator can be obtained as the second-order model multiplies with their resonance modes as shown in Fig. 2.3 and Fig. 2.4 respectively.

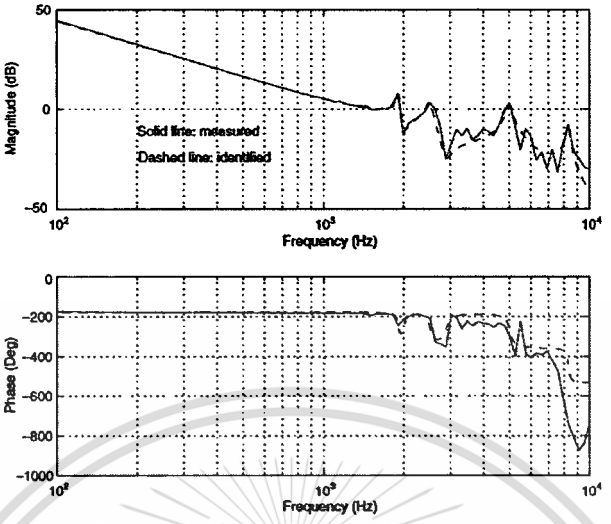

Fig. 2.3: Frequency response characteristics of the VCM [9].

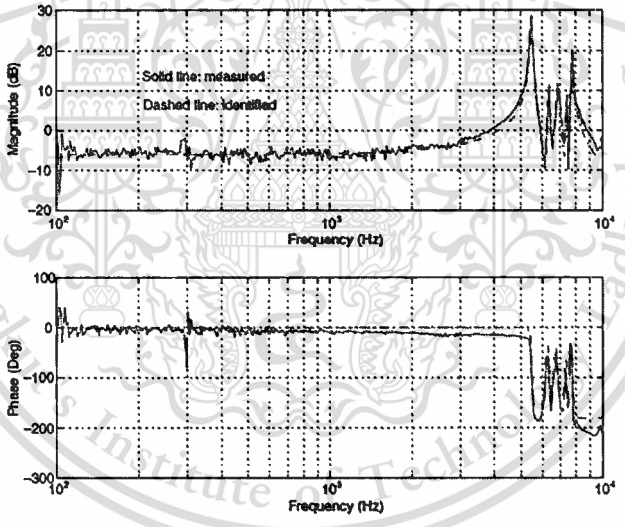

Fig. 2.4: Frequency response characteristics of the micro-actuator [9].

On the other hand, other techniques for system identification in frequency domain could also be found such as prediction error identification and a weight function matrix. It can be done in discrete-time in which the frequency data set is converted into time-domain then model can be obtained by invert discrete Fourier transform. The system identification methods can also be done in time-domain by applied impulse or step function then monitored the response [6].

2.2 Hard Disk Drive Servo Control

2.2.1 Introduction to HDD Servo Control

The task of an HDD servo system is to position the R/W head over the bits to be read or written as during the disks are spinning. HDD servo control has to move the R/W head to the desired track as fast as possible, referred as track-seeking control. The drive is in track-seeking control mode when it receive a seek command. Once the R/W head is on-track, the positioning of the R/W head on the center of the track is required as precisely as possible, referred as track-following control. When the head is positioned over the desired track, the drive switches into track-following mode then data can be read and/or written as quickly and reliably. The schematic of HDD servo system is illustrated in Fig. 2.5 [7].

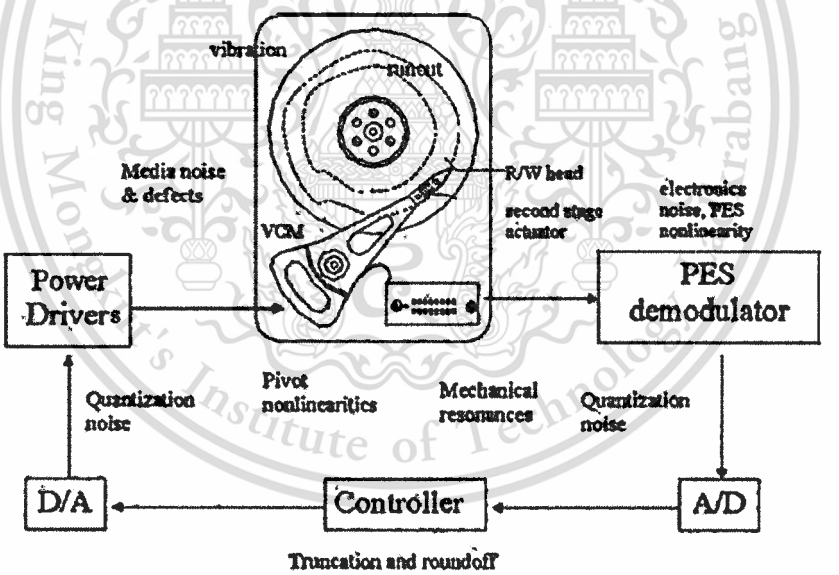

Fig. 2.5: Schematic of Closed-Loop HDD Servo Control [7].

All modern HDD, the relative position of the R/W head can be directly read from the media by using a method called embedded servo or sector servo. The implementation of the servo controller relies on the positioning error signal (PES), which is obtained by reading the position information encoded on the disk's data tracks. Each

track is further divided into sectors, using some special magnetic patterns written on the disks at the time of manufacturing. Servo patterns are created during manufacturing of the drive and the firmware of the HDD must be not to overwrite them in any situation. These special patterns are known as servo sectors which divided a track into equal segments, and data is written in these segments. The segment of the track contains the servo information in an embedded servo drive is known as servo sectors, and the section between two servo sectors is allocated for storing data bits is shown in Fig.2.6. Number of servo sectors per track is the same on all surfaces in an HDD [1], [6]-[7].

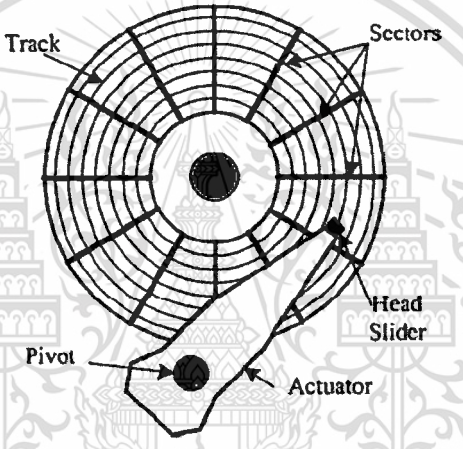

Fig. 2.6: Schematic of Tracks, Sectors and Actuator [7].

2.2.2 Track-Seeking and Track-Following on Hard Disk Drive

Both track-seeking and track-following modes use the same actuator to have the motion of R/W head to fly over the disk surface. Error tolerance during the track-following is in the scales of nanometers, and it must be achieved under the presence of various disturbances. On the other hand, the motion of R/W head from one track to another track or called track-seeking is to be performed in sub-milliseconds. Design objectives of these two modes of operation are significantly different. Besides, there must be a smooth transition between these two modes. It is impossible to meet the specifications of both modes using a single control law. Two difference controllers can also be made to produce desired performances for each task independently. However, while designing and implementing such controller, special attention must be ensure that

sudden change in the amplitude of control signal does not occur at the time of switching between modes [5]-[9], [14].

2.2.3 Source of Track Mis-Registration (TMR)

The servo system in HDD has to achieve tighter regulation control. The absolute track-following error with deviate from the center of the target track is commonly called "*track mis-registration (TMR)*". TMR is defined as the error from a nominal distance as shown in Fig. 2.7. The tracking error during regulation of head position must be less than 10% of the track pitch (distance between the two adjacent tracks), currently is in a few nanometer [1], [5]-[10].

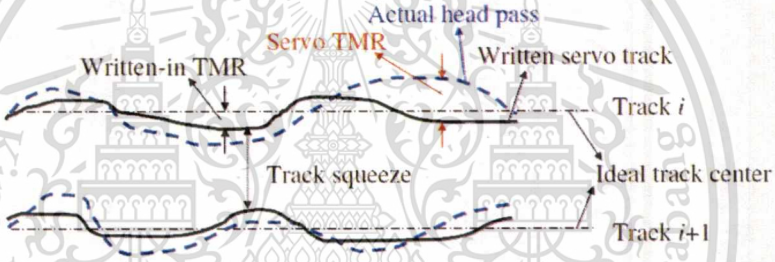

Fig. 2.7: Illustration of track mis-registration (TMR).

The disturbances affecting the performance of HDD head positioning servomechanism are contributed by some internal components of the drive as well as the external sources to the HDD, and are illustrated in Fig. 2.8. Major TMR sources are induced by internal components which consists of model mismatched, spindle runout, disk fluttering, bias force, arm and suspension vibrations due to air turbulence, PES noise, residual vibration due to seek/settling and airflow-excited suspension. The disk runout is a significant component in the TMR that can be broken down into: a repeatable runout (RRO) and a non-repeatable runout (NRRO). RRO mainly results from disk eccentricity, non-ideal servo track writing and spindle motor vibration, is hence synchronous with the disk rotation speed. All other runout other than RRO is referred to NRRO. The external disturbances are typically in the form of shocks and/or vibrations that come from the environment [1], [6]-[7].

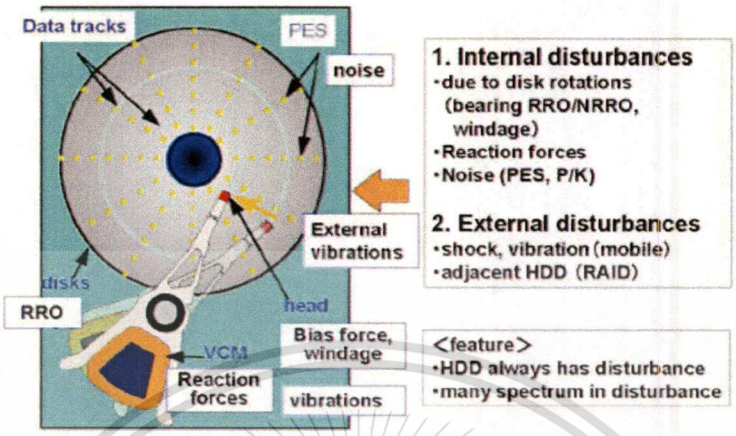

Fig. 2.8: A typical HDD indicating the various sources of TMR [1].

2.2.4 Positioning Error Signal (PES)

The position of the head is detected by the positioning error signals (PES) embedded in the data track. After assembling the HDA, the position signals are recorded on each disk by the write head using servo-writing equipment (servo track writer) in the HDD manufacturing. The position signals are recorded in a certain time interval on each track. Consequently, the position error between the head and the track can be detected directly by reading the position signal in the interval sampling period time. The position information usually consists of two parts: the coarse position giving track number and the fine position information relative to each track is shown in Fig. 2.9. Servo patterns are created during manufacturing of the drive and the firmware of the HDD and must be not overwritten in any situation. The PES represents the position difference between the center of target reference track and the R/W head position in track-following, which is measured by using of position bursts which are parts of the servo information.

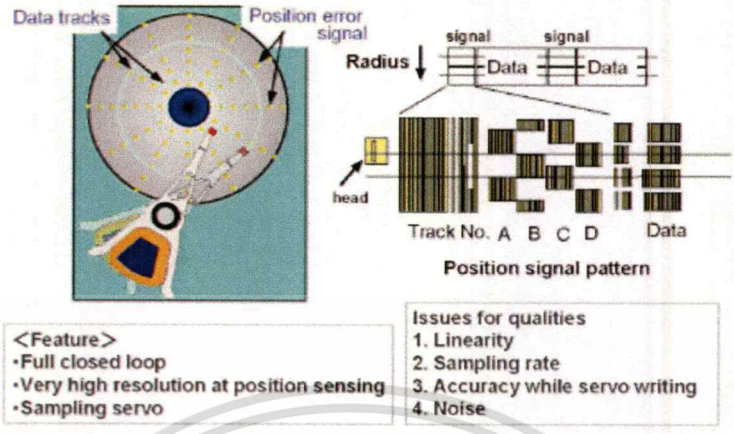

Fig. 2.9: A Typical Position Signal Pattern of HDD [1].

Track following servo systems have to ensure that the PES is kept to a minimum. The statistical distribution of the deviation measured by PES is assumed to have a Gaussian distribution and its three-times of the standard deviation $3\sigma_{PES}$ is often used to evaluate the TMR as illustrated in Fig. 2.10 [1], [6]-[7].

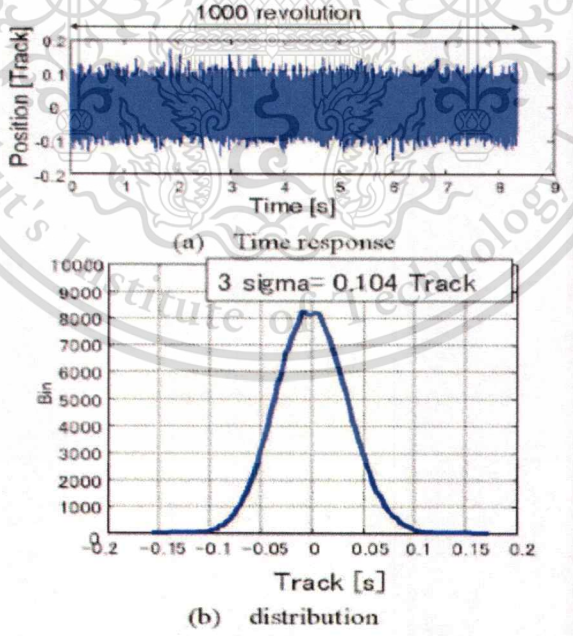

Fig. 2.10: PES Positioning Accuracy Evaluation [1].

2.2.5 Servo Bandwidth and Sensitivity Function

One of the most effective methods to reduce PES and increase precision, the servo bandwidth has to be increased in order to attend the sensitivity function ***S(s).*** The sensitivity is commonly used as the principle property to obtain the proportional-band of feedback control loop. Figure 2.11 shows the simple block diagram of an HDD servo control.

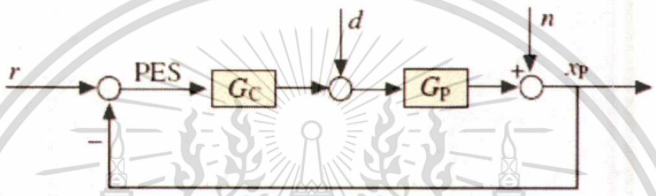

Fig. 2.11: Simple Block Diagram of HDD Servo Control [5].

$S_{(s)}$ is the closed-loop sensitivity function defined as

$$S(s) = \frac{1}{1 + G_C(s)G_P(s)}$$

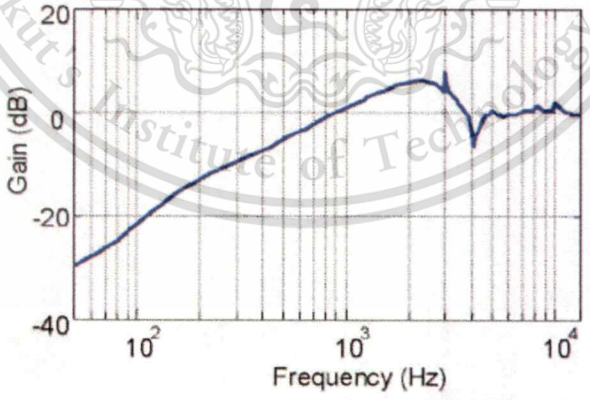

Fig. 2.12: Sensitivity Function Response [1].

An example of sensitivity function plot is illustrated in Fig. 2.12. In order to test the robustness of our design against the disturbances mentioned previously, the TMR is

input into the system, while keeping the reference signal a zero value. The expected PES in the presence of noises can be found subsequently [5]-[7].

2.3 Dual-Stage Actuator Servo Control in HDD

Various control designs have been developed for the DSA servo control and can be largely classified into two categories: the designs based on the decoupled or sequential single-input single-output (SISO), and the other ones based on modern optimal design methodologies such as linear quadratic Gaussian (LQG), loop-transfer recovery (LTR), H2/H∞ and etc. In previous studies show the both adaptive and robust control algorithms could be designed to handle external disturbance and model uncertainties. The previous studied could be found as below:

In [8], a settling control of a DSA system in HDD was presented. The mode switching was designed to switch between seeking, settling and following control together with the decoupling controller scheme. The controller was designed into three parts. The first part, the VCM feedback loop, is designed to meet the appropriate performance and stability. The second part is the PZT controller and a decoupling filter which are designed in order to achieve performance of the DSA. The decoupling filter is placed between the PZT controller output and the VCM controller input so that the PZT micro-actuator output is canceled at the VCM controller input. In the third part, the reference trajectory is designed for fast and smooth settling. The sensitivity function is used as a performance evaluation, and the gain and phase margins of the open-loop characteristic are used as stability criteria.

In [9], the design and implementation of a DSA servo system was considered. The VCM actuator was used to quickly move the R/W head of the HDD servo system to a target track, while the PZT micro-actuator was used to fine-tune the R/W head position when it was closer to the target. The composite nonlinear feedback (CNF) control, which has fast rise-time and small overshoot was designed for VCM. A simple static gain with a low-pass filter was applied for PZT micro-actuator. Simulation and implementation show significant improving in the both of settling-time and the PES tests in track-following mode.

In [10] and [11], the authors described the design of multi-input-multi-output (MIMO) approach for the HDD track-following control. A robust control design approach was based on the D-K iteration approach to μ-synthesis. The μ-synthesis required to develop a design interconnect specifying the system model, uncertainty, and weighted disturbance and penalty signals to be used by the optimization. The overall DSA system provided a high bandwidth which could be capable of very fine positioning under a various contents of disturbances.

In [12], a design of compensators for dual-input/single-output (DISO) systems was presented. The structure of a DISO system was very simpler than the structure of the general MIMO system. While the method involved the design of two SISO compensators, it was different from the master–slave technique. The proposed method eased the problem by converting control scheme into SISO design problems, which was well suited to frequency-response design techniques. The first part of the method was the design of a stabilizing compensator for an auxiliary feedback system. The second SISO compensator design was used to ensure that the feedback system was stable and then the performance and robustness specifications were achieved when evaluated in the discrete-time.

In [13], a nonlinear tracking control method for a DSA in HDD system was discussed. The design objective was to reduce the settling-time, so the VCM actuator closed-loop controller was designed with a small damping ratio for a fast rise-time and certain allowable overshoot. A composite nonlinear control law was designed for the PZT actuator to reduce the overshoot caused by the VCM actuator as the system output approached the target track. Experiments were also conducted, and the results showed a short seeking time and better track-following accuracy compared to the SSA system.

In [14], a new approach mode-switching control design in HDD servo systems was discussed. The proposed scheme used a proximate time-optimal in the track-seeking mode, and a robust perfect tracking (RPT) controller in the track-following mode. The proposed method did not require an initial value during mode switching due to some properties of the RPT controller in the secondary stage. The results of tracking error

under presence of disturbances and initial conditions showed improvement in seeking and settling-time over the conventional techniques.

In [15], two mechatronic inventions for the DSA servo system in HDD are developed. The first was the utilizing of high bandwidth DSA servo systems to improve the precision and track-following capability of the R/W head positioning control using the decoupling method. The second was the invention of the suspensions with vibration sensing strain gages acts as a vibration sensor. The proposed method could enhance the technique for tackle the problem of vibration in HDD.

In [16], a H∞ control design to achieve fast and accurate head positioning for the DSA in HDD servo system is proposed. The control scheme consisted of a tracking differentiator (TD) to avoid actuator saturation. H∞ disturbance decoupling controller dealt with the disturbances and improved the tracking performance. The simulation results in time domain and frequency domain showed that TD has provided a smooth reference signal in a feed-forward which reduced the system error, and could decrease the control effort of the both actuators. The VCM actuator was controlled by a notch filter in series with a lead compensator to stabilize the servo loop.

In [17], a discrete-time with sliding model control (SMC) design of a DSA system in HDD was considered. A state estimator based SMC was designed in the discrete time domain. The simulation results showed that the performance of the proposed technique was very fast seeking in the micro-actuator range.

In [18], an SMC based learning controller for the track-following in HDD was developed. Mathematical derivations of the control law and stability analysis were presented. The proposed controller incorporated characteristics of an SMC with the learning control. The learning algorithm utilized shape functions to approximate functions in the integral transforms and estimated the control input to reduce the repetitive error.

In [19], a discrete-time SMC scheme for a DSA tracking control system was proposed. The settling-time of the controlled system could be pre-specified by selecting a sliding hyper-plane. The results on the design of a track-seeking controller for an

optical head system showed that the proposed selecting a hyper-plane scheme provided better performance when compared to the switching controller method.

In [20], the application of a discrete-time SMC to a DSA system in HDD was described. The observer based control for the secondary actuator was incorporated with SMC. The performances for the track-seeking and track-settling process were demonstrated. The dynamics of the discrete-time SMC in state feedback controller were designed using a singular LQR approach. The proposed technique could help in reaching-phase when the states distance was far away from the sliding surface to minimize the magnitude of the control action.

In [21], a time optimal-based discrete-time SMC for HDD was developed. In this approach, an approximate time optimal switching curve was adopted for the time-varying SMC design, which consisted of an equivalent part and a discontinuous. The trajectory from any initial point was driven into a sliding region closed to the switching surface without chattering and remained there. There was the one time-varying switching surface for both track-seeking and track-following control which had provided the smooth transition. The results showed that the proposed scheme provided better performance during track-seeking than the conventional proximate time-optimal control and better for the disturbance suppression for a track-following compared to the conventional PID control.

Several architectures and design methodologies have been proposed to transform the DSA control design problem into the decoupled or the sequential multiple SISO compensator design such as a master–slave design, a decoupled design, a *PQ* method and a parallel design. The block diagram and principle of each DSA controller design will be discussed in following. The G_1 and G_2 represent the VCM actuator and the PZT micro-actuator respectively; x_1 is the position of the VCM; x_r is the position of the micro-actuator relative to the coarse actuator; x_p is the total position output; r is the reference input and is represented by the TMR in the track-following mode. The PES is the position error as $e = r - x_p$.

In master–slave structure, the absolute position error is fed to the input of PZT micro-actuator, and the output is fed to VCM actuator controller input as shown in Fig. 2.13.

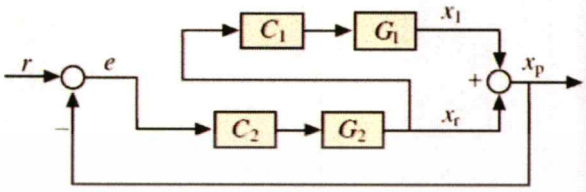

Fig. 2.13: Master–slave design structure [5].

Figure 2.14 shows the decoupled design structure. A summation of the PZT output and the error position are fed to the input of the VCM controller. The advantage feature of this structure is that the control system is decoupled into two independent control loops, and the total sensitivity function is the product of the sensitivity functions of each of the control loops. Decoupled design is also referred to as decoupled master–slave or sensitivity-function-decoupling.

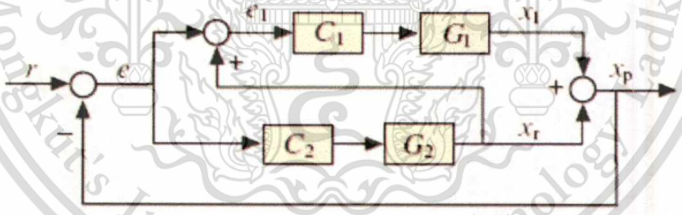

Fig. 2.14: Decoupled control design structure [5].

The *PQ* method is another control design of the DISO systems is shown in Fig. 2.15. The *PQ* design for a DSA controller can be designed in two steps. The first involves the design, *P* is defined by $P = G_1/G_2$ and an auxiliary compensator *Q* is defined by $Q = C_1/C_2$ where *Q* is designed and relative contribution of the VCM and PZT micro-actuators. The 0 dB crossover frequency and phase margin of the open-loop transfer function *PQ* are the design parameters. The second step in the *PQ* design methodology

is to design a compensator C_0. Then the bandwidth, gain margin, phase margin, and error rejection requirements of the control system are obtained.

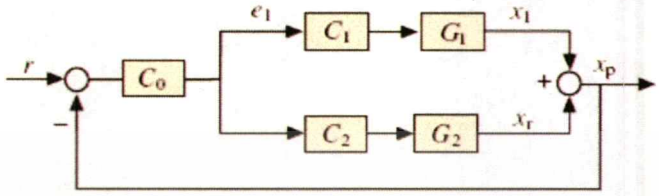

Fig. 2.15: PQ control design structure [5].

The DSA servo controller in a parallel structure is shown in Fig. 2.16. The first constraint implies that the open-loop frequency response of the DSA control system at high frequency approximately equals to the PZT control loop. Thus the compensator C_2 can be designed independently as a SISO design problem. The second constraint is to ensure that the PZT micro-actuator will not be saturated, then the compensator C_1 can be designed for the SISO plant model with the PZT closed-loop control. The advantage of this designed is to satisfy the bandwidth, gain margin, and phase margin requirements and the overall stability requirement of the DSA system.

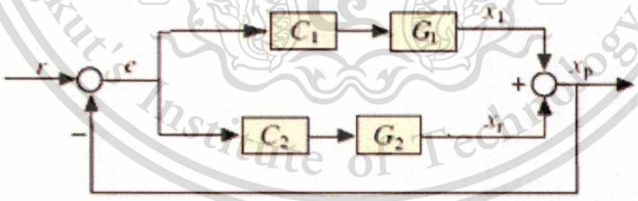

Fig. 2.16: Parallel control design structure [5].

Chapter 3
Research Methodology

In this chapter, the frequency response data are extracted from actual measuring and then mathematical modeling of the DSA system is obtained. The basic knowledge of an SMC control and enhancement of a model-reference SMC technique are also discussed in the designing of track-following servo control. This chapter describes the research methodology and is organized as follow. Section 3.1 describes the mathematical modeling of the both of VCM and PZT are obtained and validated. The basic knowledge of an SMC is discussed in Section 3.2. A model-reference SMC concept will be described in Section 3.3. Section 3.4 illustrates the research tools using in this study. It also explains the design of the proposed controller.

3.1 Dual-Stage Actuator Modeling

A DSA normally consists of two actuators: a VCM actuator and a PZT actuator as also called "PZT micro-actuator". The DSA used in this study is the suspension-based DSA which the PZT is mounted on the active suspension located between the slider R/W head and the HGA base plate. The actual measuring frequency response data of the R/W head slider motion in the DSA system are obtained in the disk drive level. The measurement is carried out to get the frequency response for each input of the DSA system. The response of the VCM is measured when the voltage of the PZT is set to zero to ensure that the PZT micro-actuator is not excited. Then the response of the PZT micro-actuator is measured while the VCM is biased with a constant current to overcome the effect of bias force. The schematic of the DSA is illustrated in Fig. 3.1. The relative distance of the R/W head output is $y = y_v + y_p$; where y_v and y_p are the linear displacements of the VCM and the PZT actuator, respectively. u_v is the voltage inputs for the VCM and u_p is the voltage inputs for the PZT micro-actuator. The frequency response data of VCM and PZT actuator can be independently shown in Fig. 3.2.

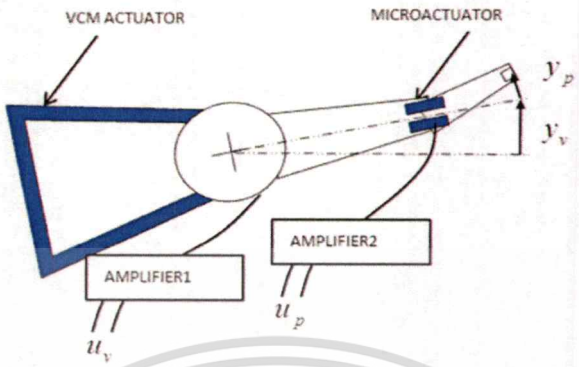

Fig. 3.1: Schematic of Dual-Stage Actuator in HDD.

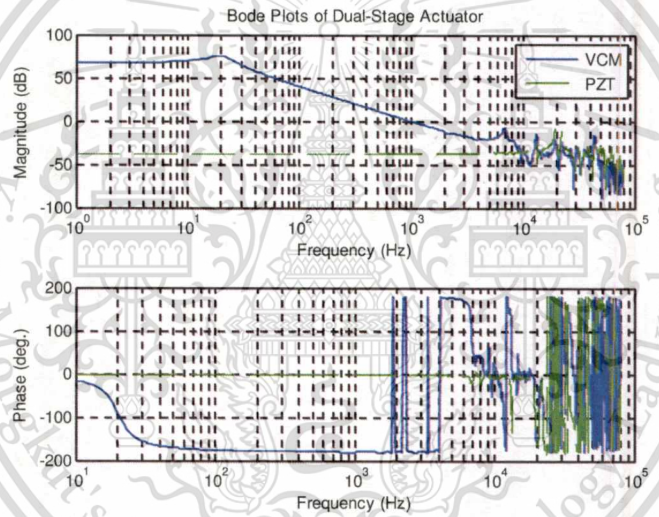

Fig. 3.2: Plots the frequency response of DSA from measurement.

The measured frequency responses obtained for the VCM shows the first peak at 6.8 KHz with multiple resonance modes thereafter. The PZT micro-actuator gain at low frequency seems constant until the first resonance peak around 13 KHz. Model fitting is done with the measuring data by using Weighted Least Square (WLS) techniques. Basics of the system identification can be found from [2]-[7] and references therein. The Matlab tools (“*ident*” and “*n4sid*”) are used for mathematical modeling estimation in the state-space form. Consequently, the continuous-time true-model transfer functions fitted for

the VCM with 20 states could satisfied the accuracy of the math model with an acceptable level of 3.77×10^{-2} model mismatch.

The PZT true-model transfer function can be estimated at 16 states with indicated the loss function at 6.7×10^{-6} could be satisfied the model mismatch. The comparison plot of the measuring data and the true-model of the VCM and the PZT are illustrated in Fig. 3.3 and Fig. 3.4 respectively.

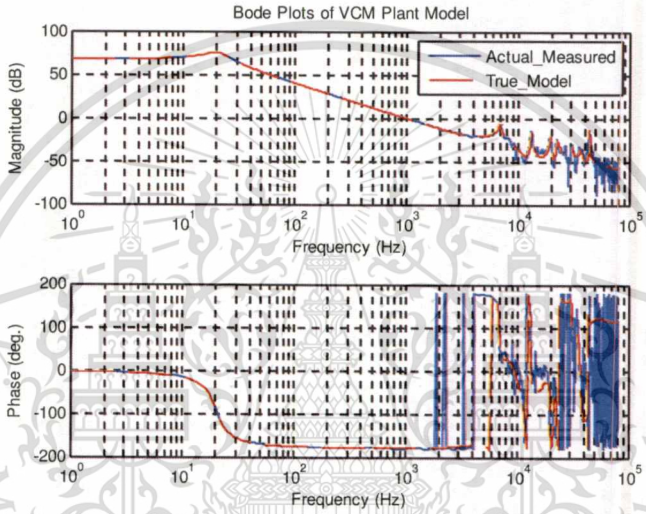

Fig. 3.3: Frequency response plots of VCM actual plant and VCM true-model.

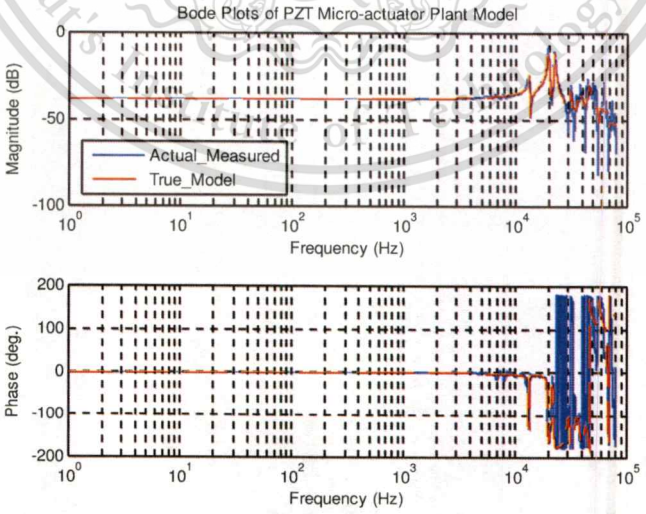

Fig. 3.4: Frequency response plots of PZT actual plant and PZT true-model.

In generally, the frequency response model of the VCM actuator and the PZT micro-actuator could expressed as the second-order model multiplies with their resonance modes. The second-order model is called a *"rigid model"* G_{ridgid}. The frequency response of the VCM and the PZT can be represented by the equations (3.1) and (3.2) respectively.

$$G_{rigid} \approx \frac{K\omega_p^2}{S^2+2\zeta\omega_p S+\omega_p^2} \tag{3.1}$$

$$\mathrm{Re}\, s \approx \prod_{i=1}^{n} \frac{S^2+2\zeta_{zi}\omega_{zi}S+\omega_{zi}^2}{S^2+2\zeta_{pi}\omega_{pi}S+\omega_{pi}^2} \tag{3.2}$$

In order to reduce the complexity of the controller design, the model order has to be reduced. We consider in the lower model order of the system order without loss of general model information such as gain and phase. The state-space model in the LTI system can be obtained in form as below:

$$\begin{aligned} x'_{(t)} &= Ax_{(t)} + Bu_{(t)} \\ y_{(t)} &= Cx_{(t)} \end{aligned} \tag{3.3}$$

where $A \in \mathbb{R}^{nxn}$, $B \in \mathbb{R}^{nxm}$, $C \in \mathbb{R}^{pxn}$, and $1 \le m < n$. The variables x is a vector of state variables, y is a vector of plant outputs, and u is a vector of control input. If the rank (B) = m and the pair (A, B) is controllable, the plant model can be transformed into the regular form as

$$\begin{aligned} \begin{bmatrix} x_1' \\ x_2' \end{bmatrix} &= \begin{bmatrix} \mathrm{A}_{11} & \mathrm{A}_{12} \\ \mathrm{A}_{21} & \mathrm{A}_{22} \end{bmatrix} \begin{bmatrix} x_1 \\ x_2 \end{bmatrix} + \begin{bmatrix} 0 \\ \mathrm{B}_2 \end{bmatrix} u \\ y &= \begin{bmatrix} \mathrm{C}_1 & C_2 \end{bmatrix} x \end{aligned} \tag{3.4}$$

where $x_1 \in \mathbb{R}^{n-m}$, $x_2 \in \mathbb{R}^m$, A_{11}, A_{12}, A_{21}, A_{22}, B_2, C_1, and C_2 are constant matrices with corresponding dimensions.

After the mathematical model is estimated as the 4th order for the VCM and the 2nd order for the PZT, the model validation is required to ensure that the estimated-model could be satisfied to represent the true-model without loss of general model information. The block diagram for model validation is illustrated in Fig. 3.5.

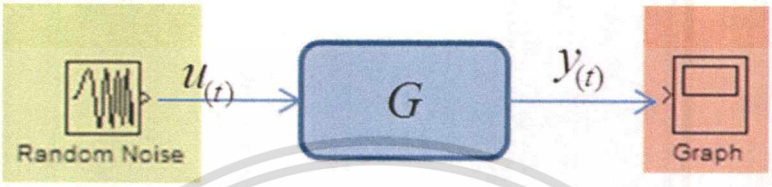

Fig. 3.5: Block Diagram for Model Validation.

In this study, the validation is done in time-domain. The random white noise in the model is replaced by the actual measured PES noise which is obtained from drive by utilizing the servo task. The PES noise with zero mean is used for the model input $u_{(t)}$ and then model output $y_{(t)}$ is monitored. The noise input is used in this study composed of the frequency spectrum up to 23 kHz which is the Nyquist frequency *(Fs/2)* when the servo sampling frequency *(Fs)* in the drive operating is 46 kHz. The input random noises in time-domain and frequency spectrum are shown in Fig. 3.6 and Fig. 3.7 respectively.

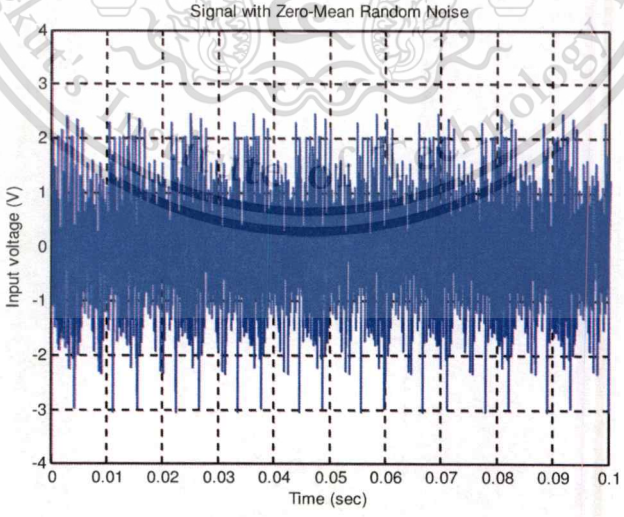

Fig. 3.6: Plots of the zero-mean random noises.

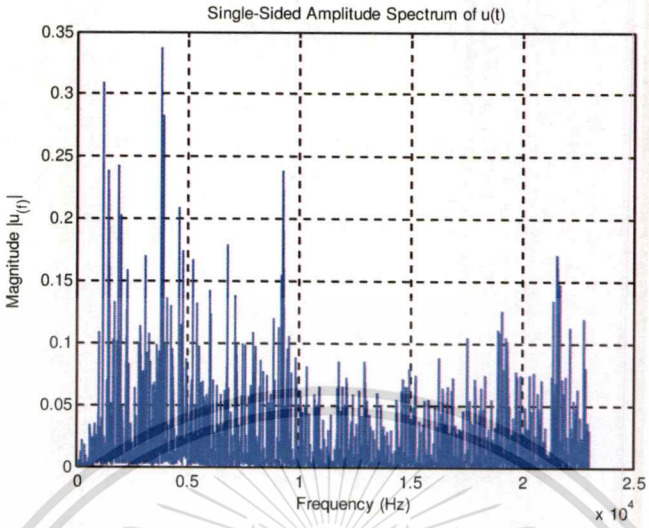

Fig. 3.7: Spectrum plot of the zero mean random noises.

The 4-states state-space model of the VCM actuator is considered in the regular form can be written as below.

$$\begin{bmatrix} x_1' \\ x_2' \\ x_3' \\ x_4' \end{bmatrix} = \begin{bmatrix} -24.6 & 123.4 & 0 & 0 \\ -123.4 & -28.8 & -3.281x10^3 & 0 \\ -0.3134 & 3.256x10^3 & -9.822x10^3 & -1.581x10^5 \\ -0.0389 & 404.8 & 1.581x10^5 & -9.817x10^3 \end{bmatrix} x + \begin{bmatrix} 0 \\ 0 \\ 0 \\ 3.536x10^3 \end{bmatrix} u_v \qquad (3.5)$$

$$y_v = \begin{bmatrix} 4.447x10^3 & -9.059 & -0.4948 & -0.5683 \end{bmatrix} x$$

The comparison of frequency response plots between the VCM 4-states model estimation and the VCM true-model is illustrated in Fig. 3.8. The model validation plot of VCM 4-states model estimation vs. the VCM true-model using random white noises is shown in Fig. 3.9. The model mismatch in the RMS error is obtained at 1.73% which is below an acceptable level at 3%.

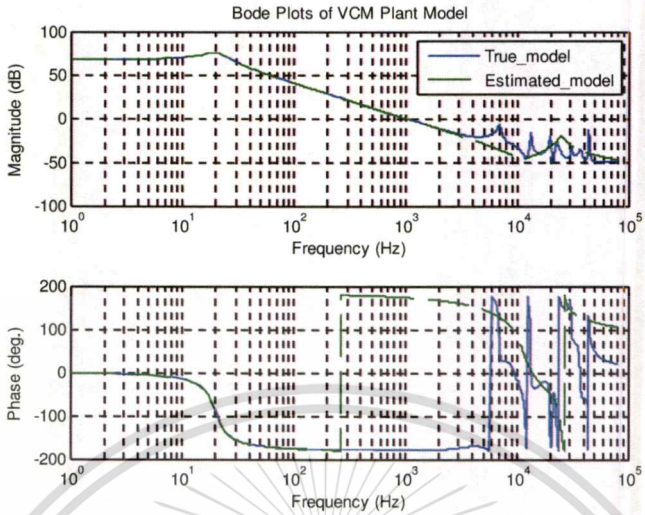

Fig. 3.8: Frequency response plots of VCM model estimation and VCM true-model.

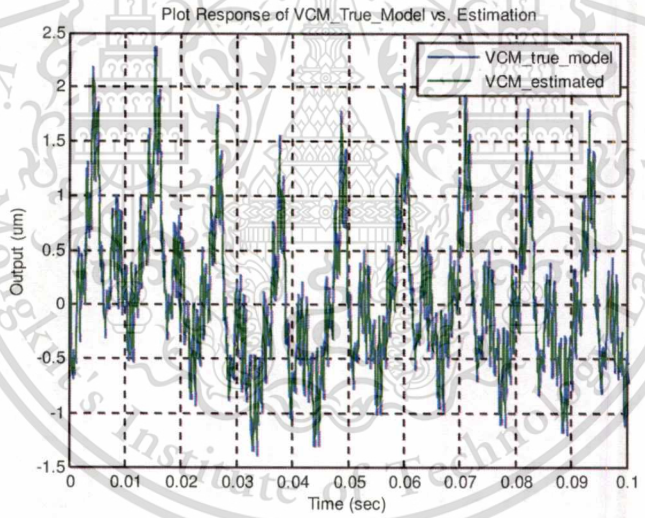

Fig. 3.9: Output response validation of VCM model estimation and VCM true-model.

And then, the second-order state-space model of the PZT can be estimated as.

$$\begin{bmatrix} x_1' \\ x_2' \end{bmatrix} = \begin{bmatrix} -3.167\text{x}10^3 & 1.323\text{x}10^5 \\ -1.323\text{x}10^5 & -3.167\text{x}10^3 \end{bmatrix} x + \begin{bmatrix} 0 \\ 37.16 \end{bmatrix} u_p \qquad (3.6)$$

$$y_p = \begin{bmatrix} 18.34 & -4.162 \end{bmatrix} x$$

The comparison plot of the PZT model estimation and the PZT true-model is illustrated in Fig. 3.10. Then, the model validation plot of the PZT model estimation and the PZT true-model is shown in Fig. 3.11. The model mismatch in the RMS error is obtained at 2.19%, and is in an acceptable level.

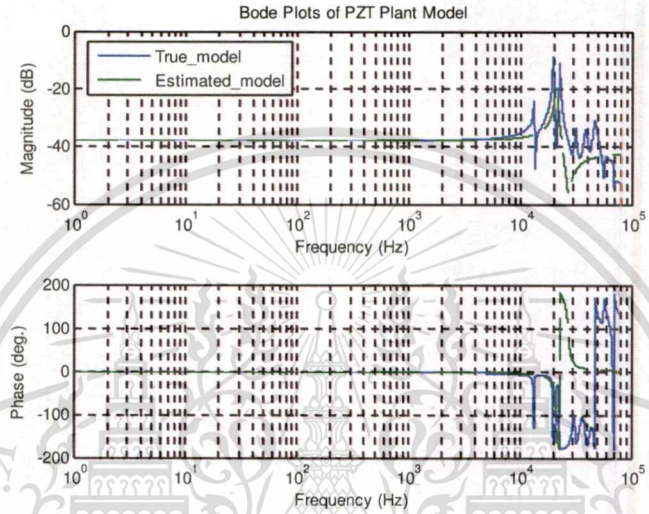

Fig. 3.10: Frequency response plots of PZT model estimation and PZT true-model.

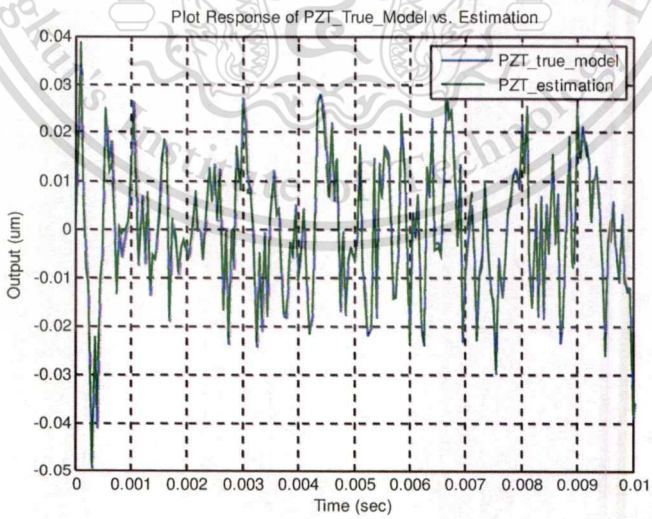

Fig. 3.11: Output response model validation of PZT model estimation vs. PZT true-model.

In summary of mathematical modeling of the DSA system, both of VCM and PZT micro-actuator are obtained. The VCM model estimation is satisfied in 4-states and the PZT micro-actuator can be defined as the second-order model. The mathematical model for both actuators satisfies function and RMS error evaluated by using the actual measured noises compared to the true-model.

3.2 Sliding Mode Control

SMC is a particular type of variable structure control (VSC) which is characterized by a suitable of feedback control law and a decision rule, normally using a switching function. The SMC design approach consists of two parts: The first involves the design of a switching function so that the sliding motion satisfies design specifications. The second is concerned with the selection of a control law which will make the switching function attracted to the system state. The basic knowledge of an SMC and some design is described in this section.

3.2.1 Principle of SMC Design

The SMC is one of the robust controller designs for nonlinear dynamic plants operating under uncertain conditions. The main advantage of the sliding mode principle is low sensitivity of plant parameter variations, model uncertainties and disturbances. Usually, SMC is considered a high-speed switching feedback control. The purpose of the switching control law is to drive the plant state trajectory onto a predetermined surface in the state-space and then to maintain the state trajectory on that surface. This surface is called the "sliding surface". The state variables are driven to a sliding surface and maintained there; this process is called "reaching phase". Once, trajectory is intercepted at the sliding surface, the switching control maintains the plant state trajectory on the surface and the state variables on the sliding surface moves to the origin, called "sliding phase". As a result, the closed-loop system dynamics are determined by the plant state trajectory restricted to the sliding surface. This section seeks to motivate and introduce

the concept which will be used in following section for DSA controller design in this study. The example to be explained using double integrator problem as given by:

$$y''_{(t)} = u_{(t)} \tag{3.7}$$

Initially, consider the effect of using the feedback control law

$$u_{(t)} = -ky_{(t)} \tag{3.8}$$

where k is a desired positive scalar. The way to analyze closed-loop motion is using phase portrait, which is the plot of the velocity against the position. Substituting the control action u in equation (3.7), multiplying the result by y', yield

$$y'_{(t)}\, y''_{(t)} = -ky'_{(t)}\, y_{(t)} \tag{3.9}$$

Integrating this expression gives the following relationship between velocity and position.

$$y'^{2}_{(t)} + ky^{2}_{(t)} = c \tag{3.10}$$

where c is a constant of integration from the initial condition. In the case if k = 1, then the equation (3.10) represents a circle with radius is $\sqrt{c}$. We need to modify the control law from equation (3.8) in order to have y and y' moves toward the origin. Consider the new control law as

$$u_{(t)} = \begin{cases} -k_1 y_{(t)} \\ -k_2 y_{(t)} \end{cases} \rightarrow \begin{matrix} if\ yy' < 0 \\ otherwise \end{matrix} \tag{3.11}$$

where $0 < k_1 < 1 < k_2$. The phase plane is partitioned by the switching rule into four quadrants as shown in Fig. 3.12. The control law $u = -k_2 y$ will be affected in the

quadrant labeled (a), likewise in region (b) when control law $u = -k_1 y$ is in operation, resulting in the distance from original point also decreases. The phase portrait of closed-loop control system in the VSC must spiral toward the origin by splicing together. The result is shown in Fig. 3.13.

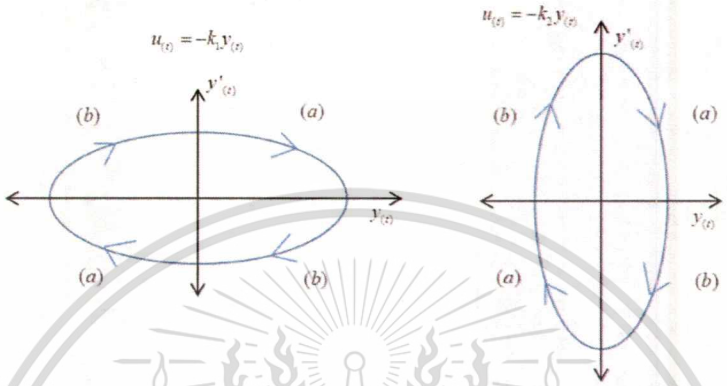

Fig. 3.12: Phase portraits of an oscillator.

Fig. 3.13: Phase portraits of the VSC system.

Sliding mode control is a special version of an on-off control. The key idea is to apply strong control action when the system deviates from the desired behaviour. The motivation of this controller is to introduce the Lyapunov function that could satisfied at

$$V_{(y)} = \frac{s_{(y)}^{\ 2}}{2} \tag{3.12}$$

where $s_{(y)}$ is the switching surface of the system. A controller will be designed in a way such that

$$V_{(y)}{}' < 0 \tag{3.13}$$

for all t. Then, the controlled system response will then be guaranteed to reach the switching surface, where $s_{(y)} = 0$, in finite value of t. We consider the switching function below which is in use at any point in the phase plane.

$$s_{(y,y')} = -my + y' \tag{3.14}$$

where m is a positive design scalar. Then define u is the signum function. Thus, can be expressed as

$$u_{(t)} = -\mathrm{sgn}(s_{(t)}) = \begin{cases} -1 & if\ s_{(y,y')} > 0 \\ 0 & f\ s_{(y,y')} = 0 \\ 1 & if\ s_{(y,y')} < 0 \end{cases} \tag{3.15}$$

It can be seen the function property as

$$s.\mathrm{sgn}(s) = |s| \tag{3.16}$$

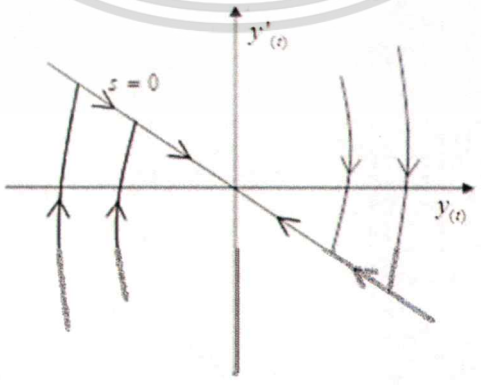

Fig. 3.14: Phase portraits of the VSC under sliding mode control [24].

From equation (3.14); when s = 0, it will be shown as straight line through the origin of gradient $-m$. as illustrated in Fig. 3.14. However, the value of y' satisfying the inequality $m|y'|<1$, then the reachability condition is satisfied as

$$ss' = s(my' + y'') = s(my' - \text{sgn}(s)) \lhd s\,|\,(m|\,y'\,|-1) < 0 \tag{3.17}$$

The motion confined to the s = 0 satisfies the differential equation by re-arranging equation (3.14)

$$y'_{(t)} = -my_{(t)} \tag{3.18}$$

This is representing the first-order decay and the trajectories will slide along the line to the origin. For example, we defined the initial condition at $y_{(0)} = 1$, $y'_{(0)} = 0$ and m =1 then the phase portrait of system behaves as a perfectly damped second-order system as shown in Fig. 3.15.

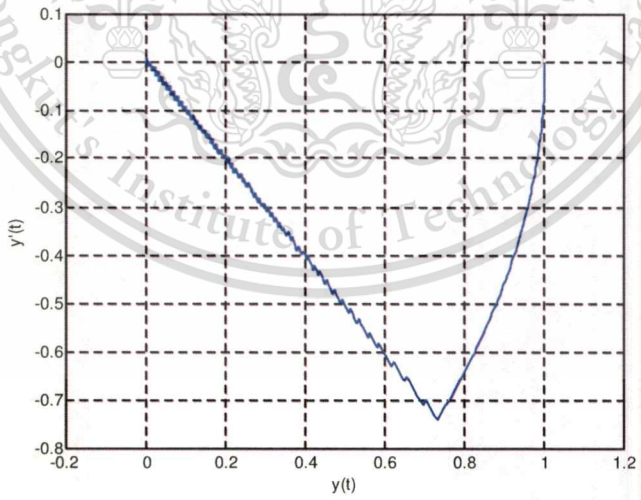

Fig. 3.15: Phase portraits of the SMC double integrator.

3.2.2 A State-Space Approach

The phase plane analysis is an effective way for second-order systems. However, multivariable system of high order will need to be analyzed in the state-space approach. We consider the double integrator once again, which can be written in state-space form as

$$\begin{bmatrix} x_1' \\ x_2' \end{bmatrix} = \begin{bmatrix} 0 & 1 \\ 0 & 0 \end{bmatrix} \begin{bmatrix} x_1 \\ x_2 \end{bmatrix} + \begin{bmatrix} 0 \\ 1 \end{bmatrix} u \tag{3.19}$$

The switching function can also be expressed in a matrix term as

$$s_{(t)} = Sx_{(t)} \tag{3.20}$$

where $S = \begin{bmatrix} m & 1 \end{bmatrix}$. Now, we consider in the normalized pendulum, can be written in the state-space form as

$$\begin{bmatrix} x_1' \\ x_2' \end{bmatrix} = \begin{bmatrix} 0 & 1 \\ 0 & 0 \end{bmatrix} \begin{bmatrix} x_1 \\ x_2 \end{bmatrix} + \begin{bmatrix} 0 \\ 1 \end{bmatrix} u - \begin{bmatrix} 0 \\ 1 \end{bmatrix} a_1 \sin(x_1) \tag{3.21}$$

It can be seen that the nonlinearity or uncertainty represented by $\sin(x_1)$ acts in the input channel, which is referred to as *"matched uncertainty"*. It was proven in literature that the VSC with the SMC control have ability to reject the effect of bounded uncertainty completely. The simulation result has attracted in detail the properties of the sliding motion and the control action, when the initial condition is defined at $y_{(0)} = 1$, $y'_{(0)} = 0$, $m = 1$ and $a_1 = 0.3$.

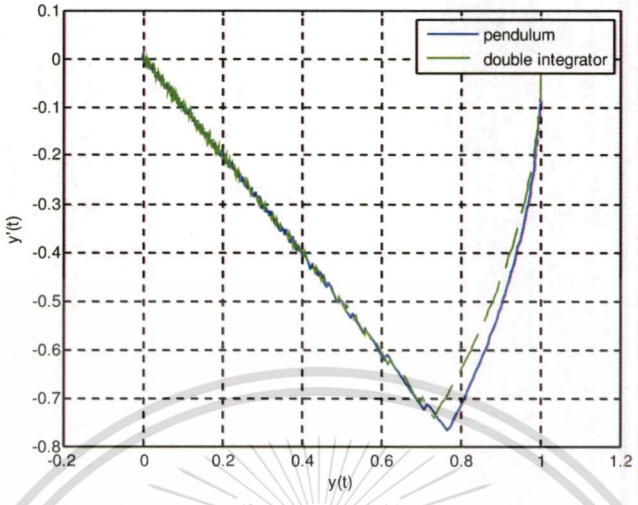

Fig. 3.16: Phase portraits of the pendulum system vs. double integrator.

Figure 3.16 shows the phase portrait that two stages nature of the dynamic is readily observed: the initial reaching phase liked a parabolic motion toward the sliding surface $s = 0$, after that followed by motion along the line toward the origin. Figure 3.17 illustrates the closed-loop behaviour for position y and the control signal u. It has shown that the VSC system from equation (3.21) is suppressed effectively. The equivalent control signal u_{eq} is shown when passed u through low pass filter.

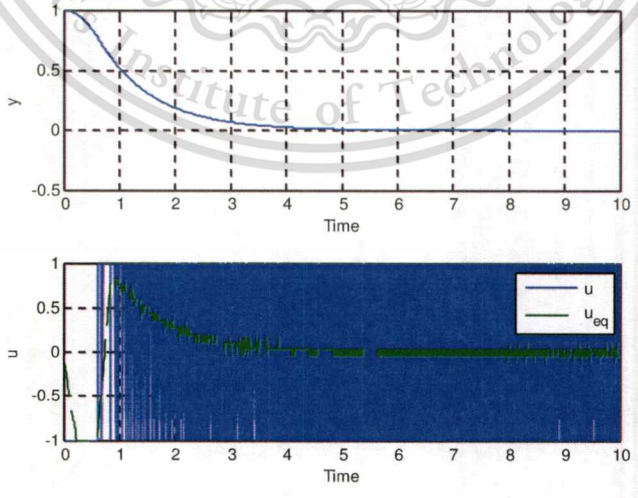

Fig. 3.17: Plots of Pendulum position (y) and control action (u) vs. time.

3.2.3 Properties of The Sliding Motion

This section describes a controller exists a sliding motion on the sliding surface. Consider the uncertain LTI system with *m* inputs given by

$$x'_{(t)} = Ax_{(t)} + Bu_{(t)} + f(t,x,u) \tag{3.22}$$

where $A \in \mathbb{R}^{n\times n}$, $B \in \mathbb{R}^{n\times m}$ and $1 \le m < n$. Without loss of generality it can be assumed that the input distribution matrix *B* has full rank. The function $f(t,x,u) \to \mathbb{R}^n$ is assumed to be unknown but bounded by some known functions of the state. Normally, the problem to be addressed is that of synthesizing a control law which forces the states back to the origin. Suppose there exists a finite time t_s such that the solution to equation (3.22) represented by $x_{(t)}$ satisfies $s_{(t)} = 0$ for all $t \ge t_s$ then an idea sliding motion is taking place. The equivalent control is the control action which is necessary to maintain an idea sliding motion on sliding surface or so called "hyper-plane". In describing the method of equivalent control it will initially be assumed that the uncertain function in equation (3.22) is to be zero. Mathematic can be expressed as $Sx_{(t)} = 0$ and $s'_{(t)} = Sx'_{(t)} = 0$ for all $t \ge t_s$, then

$$Sx'_{(t)} = SAx_{(t)} + SBu_{(t)} = 0 \tag{3.23}$$

Suppose the matrix *S* is such that the square matrix *SB* is nonsingular. Thus, the equivalent control u_{eq} associated with the nominal systems can be written as

$$u_{eq(t)} = -(SB)^{-1}SAx_{(t)} \tag{3.24}$$

The idea of sliding motion is then given by substituting the expression the u_{eq} into equation (3.22), gives

$$x'_{(t)} = (I_n - B(SB)^{-1}S)Ax_{(t)} \tag{3.25}$$

Then the eigenvectors associated with non-zero eigenvalues of the system matrix

$$A_{eq} = (I_n - B(SB)^{-1}S)A \tag{3.26}$$

From equation (3.24) the equivalent control can be considered to be the linear state feedback component necessary to reduce-order motion. It would be found that

$$u_{(t)} = -Kx_{(t)} \tag{3.27}$$

where $K = -(SB)^{-1}SA$ as a state feedback control law. The following will explain how the idea sliding motion is insensitive to the matched uncertainty function. Specifically consider the uncertain linear system given by

$$x'_{(t)} = Ax_{(t)} + Bu_{(t)} + D\xi_{(t,x)} \tag{3.28}$$

where the matrix $D \in \mathbb{R}^{nxl}$ is known matrix and the function $\xi \in \mathbb{R}^l$ is unknown. The function can be thought of representing the uncertainty or disturbance. At $s'_{(t)} = 0$ for all time $t \geq t_s$ then the control action need to maintain the motion on hyper-plane given by

$$u_{eq(t)} = -(SB)^{-1}(SAx_{(t)} + SD\xi_{(t,x)}) \tag{3.29}$$

Now, the equivalent control action is dependent on the unknown function which cannot be realized in the practical. Using the ideas of reduce-order sliding motion which is totally insensitive to the uncertain function in equation (3.28), if $\Re(D) \subset \Re(B)$. Define P_s is a projection operator as

$$P_s \stackrel{\Delta}{=} (I_n - B(SB)^{-1}S) \tag{3.30}$$

P_s satisfies the two important property of sliding motion as $SP_s = 0 \quad and \quad P_sB = 0$, then substituting the equivalent control law in equation (3.29) and equation (3.30) into the uncertain system equation (3.28), it follows that the sliding motion satisfies

$$x'_{(t)} = P_sAx_{(t)} + P_sD\xi_{(t,x)} \tag{3.31}$$

Now, supposes that, $\Re(D) \subset \Re(B)$, then the elementary column operation $\Re \in \mathbb{R}^{mxl}$ such that $D = BR$. As result it follows that $P_sD = P_s(BR) = 0$ by the projection properties. The reduced-order motion as given in equation (3.31) reduces to

$$x'_{(t)} = P_sAx_{(t)} \tag{3.32}$$

Resulting in the system does not depend on the uncertainty anymore.

3.2.4 A Regular Form Based Approach

This section will review methods for incorporating a reference signal within the sliding mode design procedure. Consider the nominal linear model of an uncertain system, given by

$$x'_{(t)} = Ax_{(t)} + Bu_{(t)} \tag{3.33}$$

where rank(B) = m, and (A,B) is controllable pair. Define an associated switching function as

$$s_{(t)} = Sx_{(t)} \tag{3.34}$$

The configuration equation (3.33) and equation (3.34) may express in the regular form

$$\begin{aligned} z_1{}'_{(t)} &= A_{11}z_{1(t)} + A_{12}z_{2(t)} \\ z_2{}'_{(t)} &= A_{21}z_{1(t)} + A_{22}z_{2(t)} + B_2u_{(t)} \end{aligned} \tag{3.35}$$

With the switch function written as

$$s_{(t)} = S_1 z_{1(t)} + S_2 z_{2(t)} \tag{3.36}$$

where the change of coordinates is defined by an orthogonal matrix T_r so that

$$z_{(t)} = T_r x_{(t)} \tag{3.37}$$

The matrix sub-blocks in equation (3.35) can be obtain in the terms of pair (A,B) from

$$T_r A T_r^T = \begin{bmatrix} A_{11} & A_{12} \\ A_{21} & A_{22} \end{bmatrix} \quad ; \quad T_r B = \begin{bmatrix} 0 \\ B_2 \end{bmatrix} \tag{3.38}$$

Likewise, the elements of the switching function in (3.36) satisfy

$$S T_r^T = \begin{bmatrix} S_1 & S_2 \end{bmatrix} \tag{3.39}$$

During sliding motion, the switching function $s(t)$ will be identically equal to zero. Thus gives.

$$S_1 z_{1(t)} + S_2 z_{2(t)} = 0 \tag{3.40}$$

This is satisfied that SB is nonsingular and implies that S_2 is also nonsingular. It can express as

$$z_{2(t)} = -M z_{1(t)} \tag{3.41}$$

where $M \in \mathbb{R}^{mx(n-m)}$ is defined to be

$$M = S_2^{-1} S_1 \tag{3.42}$$

The development of the z_2 partition in the sliding mode is thus seen to be linearly related to the z_1 partition. The sliding mode is governed by equations (3.35) and (3.41):

$$\begin{aligned} z_1{}'_{(t)} &= A_{11} z_{1(t)} + A_{12} z_{2(t)} \\ z_{2(t)} &= -M z_{1(t)} \end{aligned} \tag{3.43}$$

This is an $(n\text{-}m)^{th}$ order system in which z_2 has the role of a linear full-state feedback control signal. The equation (3.42) can be expressed as

$$z_1{}'_{(t)} = (A_{11} - A_{12} M) z_{1(t)} \tag{3.44}$$

The design requires that asymptotically stable dynamic must be ensure during sliding so that z_1 will tend to be zero as $t \to \infty$, results in giving $(n\text{-}m)$ negative poles to the closed-loop system equation (3.44). In the work, the hyper-plane matrix S will be determined from M by letting $S_2 = I_m$, giving

$$S T_r^T = \begin{bmatrix} M & S_2 \end{bmatrix} \tag{3.45}$$

This approach minimizes the calculation in proceeding from M to S thus reduces the possible of numerical errors.

3.3 A Model-Reference SMC Approach

Model following control systems theory has been developed because of the difficult in the design of multivariable control systems using linear optimal control techniques. The two major problems concerning linear optimal control because of difficulties in specifying design objectives in terms of a performance index and also due to the large variations in plant parameters which may occur. A model-reference

approach is the control system design which is able to avoid the difficulty of performance specification because the model will specify the design objectives. The controller is required to minimize the tracking error between the model and the plant. This development is so called "adaptive model following control schemes", which are required to maintain a high performance in the presence uncertainty and disturbances.

In the model-reference SMC, a reference model is relating to the plant output is predetermined. Then the SMC controller is designed with the task of the errors between the reference model state variables and the plant state variables have to be driven to zeros. As a result, the plant output is closed to the reference model output, and then specifications can be met. We consider the reference model as

$$\begin{aligned} w'_{(t)} &= A_m w_{(t)} + B_m r_{(t)} \\ y_{m(t)} &= C_m w_{(t)} \end{aligned} \tag{3.46}$$

where $A_m \in \mathbb{R}^{n\times n}$, $B_m \in \mathbb{R}^{n\times m}$ and $C_m \in \mathbb{R}^{p\times n}$, $1 \le m < n$, so the variables w is a vector of state variables, y_m is a vector of reference model outputs, and r is a vector of reference inputs. If the rank(B_m) = m and the pair (A_m, B_m) is controllable, the reference model can be transformed into regular form as

$$\begin{aligned} \begin{bmatrix} w_1' \\ w_2' \end{bmatrix} &= \begin{bmatrix} A_{m11} & A_{m12} \\ A_{m21} & A_{m22} \end{bmatrix} \begin{bmatrix} w_1 \\ w_2 \end{bmatrix} + \begin{bmatrix} 0 \\ B_{m2} \end{bmatrix} r \\ y_m &= \begin{bmatrix} C_{m1} & C_{m2} \end{bmatrix} w \end{aligned} \tag{3.47}$$

where $w_1 \in \mathbb{R}^{n-m}$, $w_2 \in \mathbb{R}^m$, A_{m11}, A_{m12}, A_{m21}, A_{m22}, B_{m2}, C_{m1}, and C_{m2} are constant matrices with corresponding dimensions. The reference model (A_m, B_m) can be formulated so that the model outputs y_m follow the reference inputs r with desirable transient response. One way to find the matrices A_m and B_m is to use pole-placement method. Define a tracking error state e as the error between the plant state variables and the reference model state responses:

$$e_{(t)} = x_{(t)} - w_{(t)} \tag{3.48}$$

This error is required to tend asymptotically to zero. Differentiating the error equation (3.48) with respect to time yields the error dynamics is given by

$$e'_{(t)} = x'_{(t)} - w'_{(t)} \tag{3.49}$$

The dynamics of the model-following error system can now be determined as

$$e'_{(t)} = A_m e_{(t)} + (A - A_m)x_{(t)} + Bu_{(t)} - B_m r_{(t)} \tag{3.50}$$

A sufficient condition is that all orders of time derivatives of the error are zero at any time *t*. It follows that $x_{(t)} = w_{(t)}$. The whole design of an SMC system is to properly choose or design a sliding surface, that the closed-loop system has desired dynamics. And then a switching control that can drive the plant state trajectory onto the sliding surface and maintain it on that surface is to be designed. The control inputs *u* will make *x* tracks *w,* corresponding to *y* tracks y_m.

If we want to design *u* for the plant model equation (3.33) to have desirable closed-loop poles and to ensure steady-state tracking is zero, we choose

$$u_{2(t)} = Fx_{(t)} + Gr_{(t)} \tag{3.51}$$

Then, the closed-loop system becomes

$$\begin{aligned} x'_{(t)} &= (A + BF)x_{(t)} + BGr_{(t)} \\ y_{(t)} &= Cx_{(t)} \end{aligned} \tag{3.52}$$

Then the transfer function from *r* to *y* is given by

$$\frac{y_{(s)}}{r_{(s)}} = C\left(sI - \left(A + BF\right)\right)^{-1} BG$$
$$G = -\left(C\left(A + BF\right)^{-1} B\right)^{-1} \tag{3.53}$$

Consider a control law

$$u_{(t)} = u_{1(t)} + u_{n(t)} + u_{2(t)} = v_{(t)} + u_{2(t)} \tag{3.54}$$

where

$$u_{2(t)} = B^{\dagger}(A_m - A)x_{(t)} + B^{\dagger}B_m r_{(t)} \tag{3.55}$$

u_2 is an inverse dynamics term with $B^{\dagger}$ as pseudo-inverse of B. Substituting equation (3.54) into equation (3.50), gives

$$e'_{(t)} = A_m e_{(t)} + Bv_{(t)} \tag{3.56}$$

Since both plant model and reference model are in regular form, the error dynamics can also be written in regular form as

$$e_1{}'_{(t)} = A_{m11}e_{1(t)} + A_{m12}e_{2(t)}$$
$$e_2{}'_{(t)} = A_{m21}e_{1(t)} + A_{m22}e_{2(t)} + B_2 v_{(t)} \tag{3.57}$$

Suppose A, B, A_m and B_m satisfy the perfect model-matching conditions. If x and r are considered to be disturbances to the error dynamic, then the perfect model-matching conditions guarantee that the behaviour of the VSC in the SMC is insensitive to these disturbances. In SMC, the error system is equivalent to a system of order (n-m). Let the switching surface be

$$s_{(t)} = Se_{(t)} = S_1 e_{1(t)} + S_2 e_{2(t)} = S_2 M e_{1(t)} + S_2 e_{2(t)} \tag{3.58}$$

where S, S_1, S_2, and M are constant matrices with appropriate dimensions. Let S_2B_2 is any non-singular diagonal matrix, normally chosen to be B_2 so that $S_2 = I$. Using a linear change of coordinates

$$T_s \overset{\Delta}{=} \begin{bmatrix} \mathrm{I} & 0 \\ \mathrm{S}_1 & \mathrm{S}_2 \end{bmatrix}, \text{ we have } \quad \begin{bmatrix} e_1 \\ s \end{bmatrix} = T_s \begin{bmatrix} e_1 \\ e_2 \end{bmatrix} \tag{3.59}$$

Choose

$$u_{l(t)} = -(SB)^{-1}(SA_m - \Phi S)e_{(t)} \tag{3.60}$$

where Φ is any stable design matrix, and then choose

$$u_{n(t)} = -\rho(SB)^{-1}\frac{P_2 s_{(t)}}{\left\| P_2 s_{(t)} \right\|} \tag{3.61}$$

where $\rho > 0$ is a design parameter and P_2 is a symmetric positive definite matrix equation

$$P_2\Phi + \Phi^T P_2 = -I \tag{3.62}$$

After a straight-forward derivation, we obtained

$$e_1{}'_{(t)} = \left(A_{m11}e_{1(t)} - A_{m12}M\right)e_{1(t)} + \left(A_{m12}S_2{}^{-1}\right)s_{(t)} \tag{3.63}$$

$$s'_{(t)} = \Phi s_{(t)} - \rho\frac{P_2 s_{(t)}}{\left\| P_2 s_{(t)} \right\|} \tag{3.64}$$

Consider a Lyapunov function $V_1 = s^T P_2 s > 0$, so the derivative is given by

$$\begin{aligned} V_1' &= s^T{}' P_2 s + s^T P_2 s' \\ &\le \|s\|^2 - 2\rho \|P_2 s\| \\ &\le -2\rho \sqrt{\lambda_{\min} P_2} \sqrt{V_1} \\ &\le 0 \end{aligned} \tag{3.65}$$

From the Rayleigh principle, we can conclude that s will approach zeros in finite time and will remain there afterward. M to be defined and $(A_{m11} - A_{m12}M)$ is a stable matrix. So that we can conclude that e_1 will approach zeros in finite time and during time $s = 0$, the result in e_2 will also approach zeros.

In summary, the model-following design objective is to develop a control scheme which forces the plant states to follow the dynamics of an ideal model. The controller will force the error between the plant system and the reference model states to zero. This will ensure that the plant system output follows the reference model output accordingly. If the control law is properly designed then the perfect model-matching conditions guarantee that the behaviour of the VSC system in the SMC is insensitive to the model uncertainty and disturbances.

3.4 Dual Stage Actuator Design Approach

In this study, the block diagram of the overall control system of the DSA is proposed as illustrated in Fig. 3.18. This is based on the decoupling scheme. The controller design requires that the PZT micro-actuator must settle down to zero before its next move. A model-reference sliding model control (MRSMC) is used in this study.

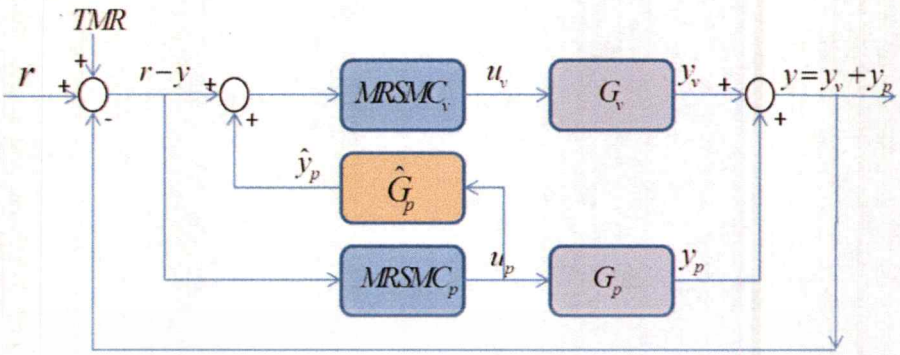

Fig. 3.18: Schematic diagram of DSA control.

The DSA control loop from r to y consists of the following components. G_v is the VCM plant that in the practical can be considered in a series with desired notch filter for system stabilizing. $MRSMC_v$ is the designed controller for the VCM actuator plant. Gp is plant of the PZT micro-actuator that can also be considered to connect in a series with notch filter for improving stability of the system in the practical. $MRSMC_p$ is the designed controller of the PZT plant. The block $\hat{G}_p$ is the decoupling filter, which is placed between the VCM controller input and the PZT controller output. The PZT micro-actuator output is cancelled at the VCM controller input. We can define that $\hat{y}_p \cong y_p = y - y_v$. The signal r represents the input commands for DSA servo control to move the head and position onto the target track. Let $r-y$ is to be the controller input of PZT micro-actuator. Then $r-y_v$ is to be the input to the VCM controller, which is suitable for the regulation control problem. The advantage features of this structure is that the control system is decoupled into two independent control loops, and the total sensitivity function is the product of the sensitivity functions of each control loop can be referred as

$$S = \frac{1}{1+Go} = \frac{1}{(1+MRSMCv.Gv)} \cdot \frac{1}{(1+MRSMCp.Gp)}.$$

During operation, only total of the head displacement $y = y_v + y_p$ is measured; y_v and y_p are not directly measured. To obtain feedback displacement, we used the fact that the PZT micro-actuator can be accurately approximated as $\hat{G}_p \cong G_p$. Therefore,

we have $\hat{y}_p = \hat{G}_p u_p \cong y_p$ and $\hat{y}_v = y - \hat{y}_p$. Both $\hat{y}_v$ and $\hat{y}_p$ can be used as approximated displacements of the feedback control system. Based on the fact that the PZT micro-actuator can be accurately approximated by a constant gain under present the range of operating frequency.

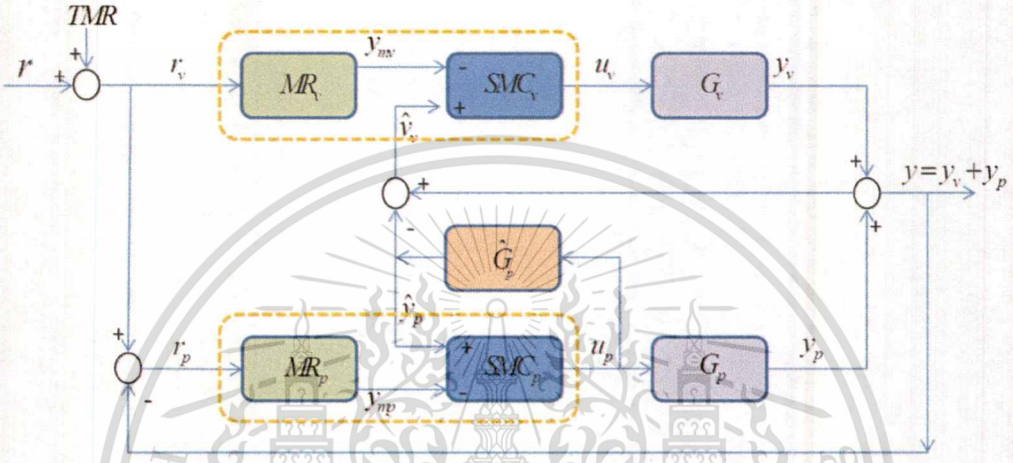

Fig. 3.19: Schematic diagram of MRSMC for the DSA.

Figure 3.19 contains block diagram of overall MRSMC control system as following:

- MR_v is the reference model of the VCM actuator.
- MR_p is the reference model of the PZT micro-actuator.
- SMC_v is the sliding mode controller design for the VCM actuator.
- SMC_p is the sliding mode controller design for the PZT micro-actuator.
- G_v is the actual plant of the VCM actuator.
- G_p is the actual plant of the PZT micro-actuator.
- $\hat{G}_p$ is the decoupling filter.
- r is the reference input command to the controller.
- r_v is the input to the reference model of the VCM.
- r_p is the input to the reference model of the PZT.
- y_{mv} is the output of the reference model of the VCM.
- y_{mp} is the output of the reference model of the PZT.

- u_v is the output of the SMC controller of the VCM or control signal to the VCM plant.
- u_p is the output of the SMC controller of the PZT or control signal to the PZT plant.
- y_v is the output displacement of the VCM plant.
- y_p is the output displacement of the PZT.
- y is the total output displacement of the head.
- $\hat{y}_v$ is the estimated output displacement of the VCM.
- $\hat{y}_p$ is the estimated output displacement of the PZT.

The reference input for the VCM actuator is $r_v = r$, whereas the reference input of the PZT micro-actuator is $r_p = r - y$. This is to fulfil the requirement that the PZT micro-actuator is working to compensate in the tracking error and must settle down to zero in the steady-state before next move. The reference models for each actuator could be designed independently. For the SMC controller with a model-reference approach, the error between the reference model output and the plant output is fed into the SMC controller in order to enforce the plant state to track the reference model. This is satisfied that $y_{mv} - \hat{y}_v$ is the input fed into the ***SMCv***, while $y_{mp} - \hat{y}_p$ is for SMC_p.

In the track-following task DSA servo control task, r is replaced by TMR to be the input to the controller. Normally, TMR consists of the repeatable run out (RRO), non-repeatable run out (NRRO) and external disturbances. The PES is the position error, $e = r - y$.

The objective of a model-reference SMC designs for the DSA system is to have the displacement of the head tracks a reference command. The following specifications have to be met:

- The mean of the steady-state error is zero.
- The 3σ PES is to be less than 10% of track width under present TMR disturbances.
- The 5% settling-time of step response is to be short as short as possible and the overshoot and undershoot is to be less than 5%.

- The micro-actuator must settle down to zero in the steady state for further the next move.
- The displacement of the PZT micro-actuator does not exceed 0.5 um which is the maximum displacement specification of the PZT.

3.4.1 Design of Reference Model for the DSA System

The first task of designing a model-reference SMC is to design the reference models for both actuators. Equation (3.5) and (3.6) represent the mathematical model for the VCM and the PZT micro-actuator respectively. Equation (3.51) and (3.52) are referred as the closed-loop reference models. A full-state feedback matrix *F* can be designed to place the closed-loop poles at desired locations to achieve desirable transient response. To ensure steady-state tracking of a step reference, using the final-value theorem. Therefore, the reference model can be chosen as

$$\begin{aligned} A_m &= (A + BF) \\ B_m &= BG \end{aligned} \tag{3.66}$$

The reference models for both actuators are found by placing the poles of (*A, B*). The desired poles at [*-1x10^4, -1.2x10^4, -1.8x10^4, -2x10^4*] are placed for the VCM system model, then the closed-loop model-reference of the VCM can be found as

$$\begin{bmatrix} x_1' \\ x_2' \\ x_3' \\ x_4' \end{bmatrix} = \begin{bmatrix} -24.6 & 123.4 & 0 & 0 \\ -123.4 & -28.8 & -3.281x10^3 & 0 \\ -0.3134 & 3.256x10^3 & -9.822x10^3 & -1.581x10^5 \\ -6.698x10^5 & -2.289x10^4 & 5.121x10^3 & -5.013x10^4 \end{bmatrix} x + \begin{bmatrix} 0 \\ 0 \\ 0 \\ 151.8 \end{bmatrix} u_v \tag{3.67}$$

$$y_v = \begin{bmatrix} 4.447x10^3 & -9.059 & -0.4948 & -0.5683 \end{bmatrix} x$$

The desired poles at [*-1.1x10^4, -2x10^4*] are placed to get the closed-loop reference model of the PZT micro-actuator, and the PZT reference model is shown as

$$\begin{bmatrix} x_1' \\ x_2' \end{bmatrix} = \begin{bmatrix} -3.167\text{x}10^3 & 1.323\text{x}10^5 \\ -996.6 & -2.783\text{x}10^4 \end{bmatrix} x + \begin{bmatrix} 0 \\ 91.18 \end{bmatrix} u_p \qquad (3.68)$$
$$y_p = \begin{bmatrix} 18.34 & -4.162 \end{bmatrix} x$$

To ensure that the closed-loop reference models could be satisfied the steady-state tracking error of a square wave reference input ***r***. The simulation plot of reference model output tracking for the VCM is shown in Fig. 3.20. The simulation plot of reference model output tracking for the PZT micro-actuator is shown in Fig. 3.21. Both are satisfied in the settling-time, overshoot and undershoot.

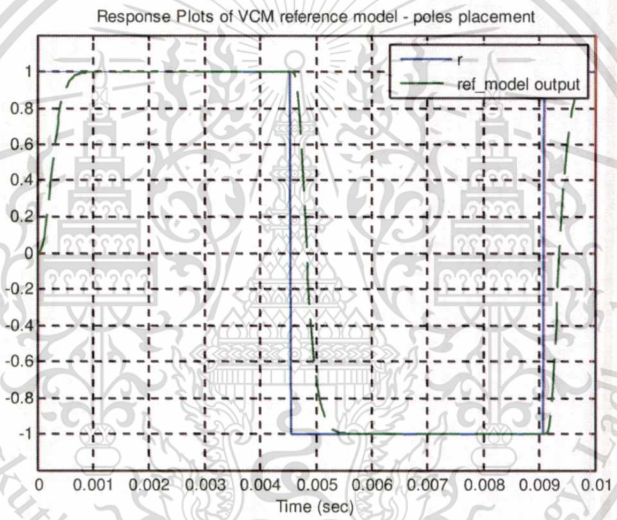

Fig. 3.20: Output response tracking of the reference model for the VCM.

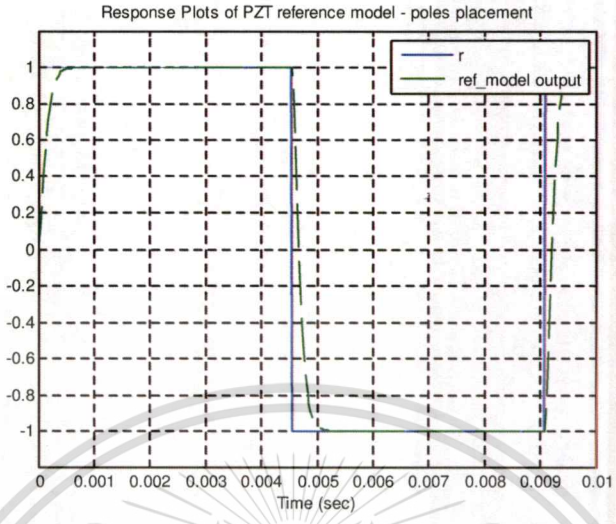

Fig. 3.21: Output response tracking of the reference model for the PZT.

We can see that the desired closed-loop reference models using the final-value theorem for the both of VCM and PZT actuator are satisfied of meeting the time domain specification requirements such as the steady-state error, the settling time is shorter than 0.5 msec. and the overshoot is less than 5%.

3.4.2 A Model-Reference SMC Closed-Loop Controller Design Approach

Consider the system in the regular form by the equation (3.38). We can design the control system for the VCM actuator referred equation (3.5) and the PZT micro-actuator referred equation (3.6) accordingly. The system for the both of VCM and PZT can be partitioned as equation (3.69) and (3.70) respectively.

$$\left[\begin{array}{c|c} A_{11} & A_{12} \\ \hline A_{21} & A_{22} \end{array}\right]_{vcm} = \left[\begin{array}{ccc|c} -24.6 & 123.4 & 0 & 0 \\ -123.4 & -28.8 & -3.281x10^{3} & 0 \\ -0.3134 & 3.256x10^{3} & -9.822x10^{3} & -1.581x10^{5} \\ \hline -0.0389 & 404.8 & 1.581x10^{5} & -9.817x10^{3} \end{array}\right] \tag{3.69}$$

$$\left[\begin{array}{c|c} A_{11} & A_{12} \\ \hline A_{21} & A_{22} \end{array}\right]_{pzt} = \left[\begin{array}{c|c} -3.167x10^{3} & 1.323x10^{5} \\ \hline -1.323x10^{5} & -3.167x10^{3} \end{array}\right] \tag{3.70}$$

In the thesis study, the switching function matrix S will be determined according to equation (3.45). In general, let S_2B_2 is any non-singular diagonal matrix by chosen $S_2 = -I_m$, gives

$$S = \begin{bmatrix} M & | & -I_m \end{bmatrix} \tag{3.71}$$

By referring the equation (3.44), the design requires asymptotic stable. The method considered here is based on robust poles placement, results in giving (n-m) negative poles to the closed-loop system. Then the matrix M for VCM is constructed by placing the poles of (A_{11}, A_{12}) at [$-1x10^3$, $-2x10^3$, $-3x10^3$], then the switching function for the VCM system is

$$S_{vcm} = \begin{bmatrix} -0.0882 & 0 & -0.0245 & | & -1 \end{bmatrix} \tag{3.72}$$

The pole at [$-2x10^3$] is placed for PZT micro-actuator system. Then the switching function for the PZT micro-actuator loop is obtained as

$$S_{pzt} = \begin{bmatrix} -0.0088 & | & -1 \end{bmatrix} \tag{3.73}$$

Next, the task of MRSMC designing is to consider a control law according to the equation (3.54), which is formulated from the equations (3.55), (3.60) and (3.61). The designed parameters P_2, Φ and ρ have to be considered. In the practical, P_2 is set to be I_m, then Φ can be obtained by solving the Lyapunov function which satisfies $\Phi = 1$. Normally, the parameter ρ is set to 1. The simulation results can be discussed in the following chapter.

Chapter 4
Results and Discussions

In this chapter, the results of the proposed technique MRSMC for the DSA track-following servo control are compared to the time-domain specified performance criteria. The 3σ PES for tracking error performance of the control system is evaluated as the actual measured TMR sources in disk drive operating is used for evaluation. The settling-time and overshoot are obtained from step response. The chattering reduction is also discussed. The performances of proposed technique in the DSA system controller design are compared with the SSA system and also compared with the conventional PID technique.

4.1 Tracking Error Validation

This section describes the simulation results of the tracking performance of the proposed controller in the DSA system. The RRO source in equation (4.1) is used for this evaluation is referred from [6]. This is the normalized value which is obtained by dividing the position by the track width (*position/trackwidth*). The normalized reference position is set at 0.5 which is equivalent to the center of the track. It composes 55 Hz fundamental frequency along with other harmonics frequencies. The tracking result could be satisfied and is shown in Fig. 4.1.

$$r_{TMR}(t) = 0.5 + 0.1\cos(110\pi t) + 0.05\sin(220\pi t) + 0.02\sin(440\pi t) + 0.01\sin(880\pi t) \qquad (4.1)$$

The tracking error of a proposed technique in the DSA track-following system is illustrated in Fig. 4.2. It can be seen that the preliminary results could be satisfied.

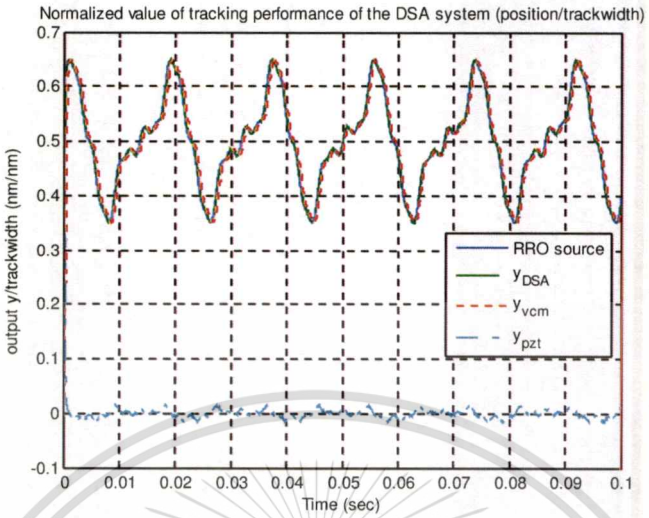

Fig. 4.1: Plots of tracking performance of the DSA system.

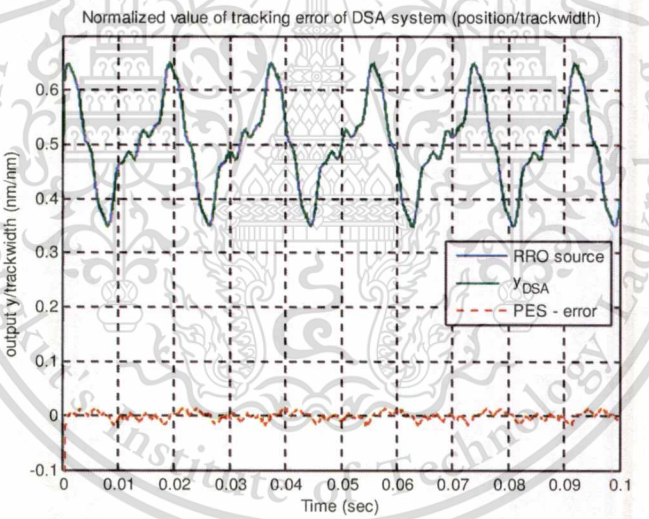

Fig. 4.2: Plots of tracking error of the DSA system.

4.2 Positioning Error Evaluation – PES Testing

This section describes the PES testing results of the proposed design in the DSA tracks-following servo control. The 3σ PES is used to compare and evaluate the tracking error performance which represents the position of the R/W head deviated from the

center of the track. The relative sampling frequency ***Fs*** for the servo controller is normally defined by:

$$Fs = RPM * Wage \tag{4.2}$$

where ***RPM*** is the speed of spindle motor per second and ***Wage*** is the number of servo sectors per track. The configurations setup in this simulation is referred as follow. The spindle motor speed (***RPM***) is 5400 rpm, the servo encoding (***Wage***) is 512 per track. Then, the relative servo sampling frequency (***Fs***) is 46.08 kHz.

In the track-following DSA servo control, r is set to zero then the TMR is represented the input to the controller. The TMR disturbances used in this study is obtained from the actual measurement. The measured TMR from the disk drive is illustrated in Fig. 4.3 and the spectrum of the TMR sources is shown in Fig. 4.4. It can be seen that the fundamental frequency is of the spindle rotation speed at 90 Hz, which mean that RRO is the dominant source of TMR.

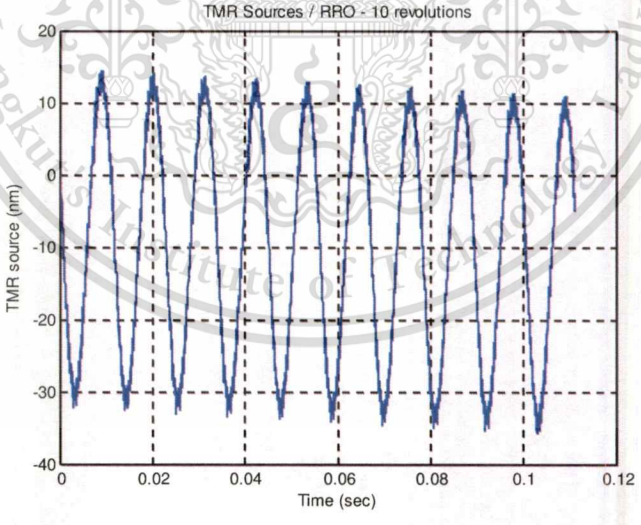

Fig. 4.3: Plots of Actual Measured TMR Sources in Disk Drive.

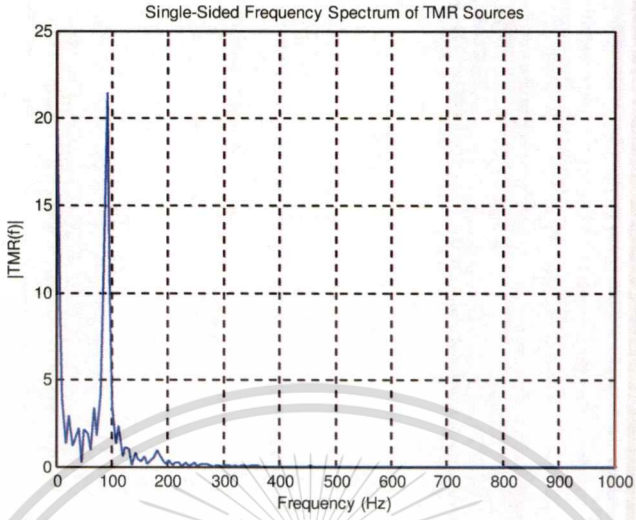

Fig. 4.4: Spectrum Plots of Actual TMR Sources.

We are now considering of the performance comparison between the DSA systems and the SSA system using the same proposed design technique. In fact, the SSA is a subsystem of the DSA system. SSA can be utilized by disabling the blocks of the PZT micro-actuator paths from the DSA control scheme. Therefore, the SSA is a simple SISO control system. We have to re-design the control parameters suitable for the SSA system. The reference model is defined by referring from the equation (3.66). The closed-loop poles of the SSA reference model are desired by placing the system poles of (A, B) at location $[-1x10^4, -1.5x10^4, -2x10^4, -2.5x10^4]$. The control law design of the SSA is referred to the VCM model using in the DSA system as in equation (3.54). The switching function is supposed not to be changed as referred to equation (3.27). The rest of designed parameters are the same as being used in the DSA system, in which P_2 is set to I_m, Φ and ρ are set to 1. Then the simulation results of DSA and SAA systems are compared. The results of tracking performances of the DSA and SSA are shown in Fig. 4.5. The PES off-tracks of both systems are illustrated in Fig. 4.6 and the 3σ PES positioning errors are shown in Fig. 4.7.

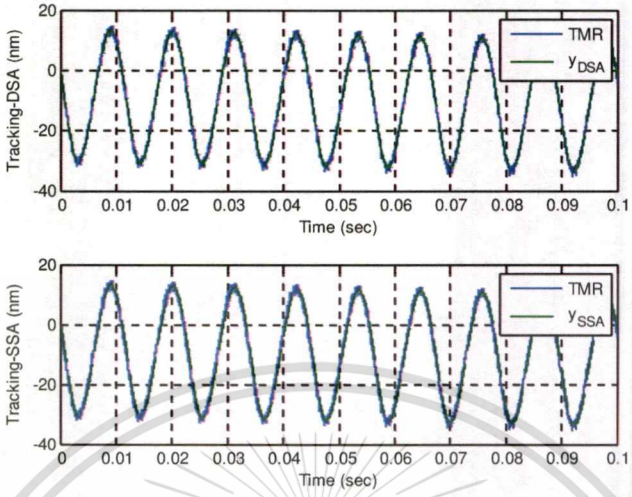

Fig. 4.5: Comparison of tracking performance using a model-reference SMC in DSA vs. SSA.

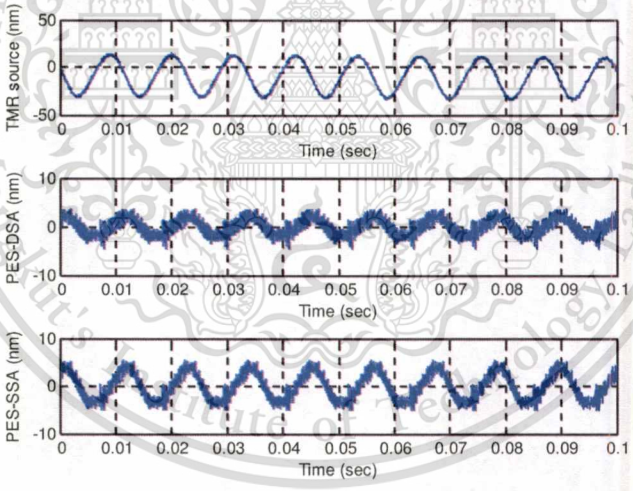

Fig. 4.6: Comparison of PES - tracking error using a model-reference SMC in DSA vs. SSA.

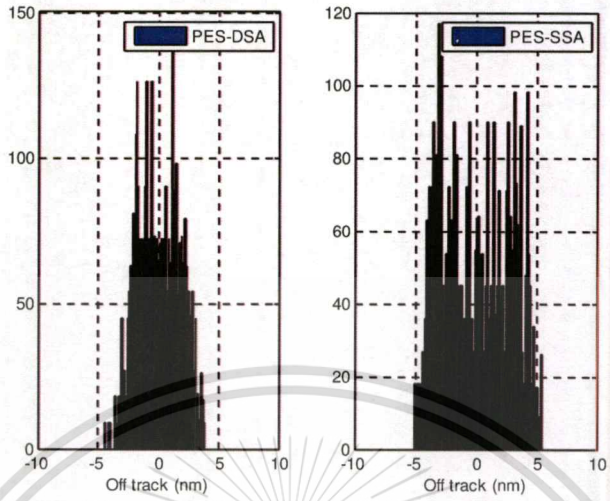

Fig. 4.7: Comparison of PES off-track (3σ) using a model-reference SMC in DSA vs. SSA.

The tracking response of the DSA track-following servo system is illustrated in Fig. 4.8. It can be seen that the proposed controller design using a model-reference could be satisfied with the tracking error requirements and met the performance specifications. Result of the 3σ PES off-track testing of the DSA system is 5.16 nm which is 38.3% better than the SSA system at 8.36 nm.

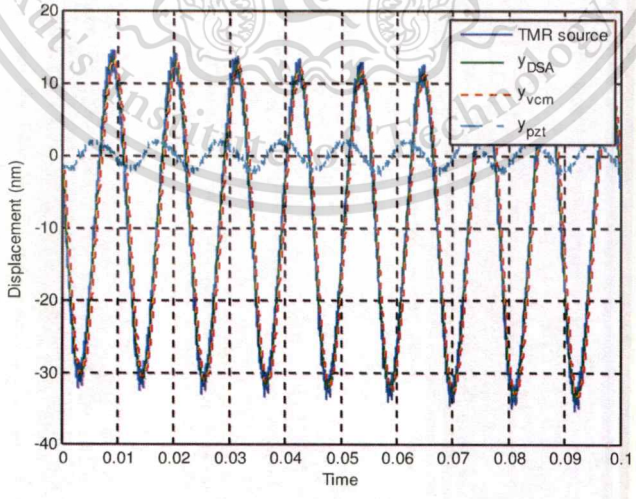

Fig. 4.8: Responses of the DSA track-following servo system under present TMR.

4.3 Step Responses Evaluation

This section describes the simulation results of the proposed controller design when input command is the unit step function. The time-domain specifications are evaluated by applying the reference at 100 nm which is equivalent to the track width. The step response of the DSA system is illustrated in Fig. 4.9.

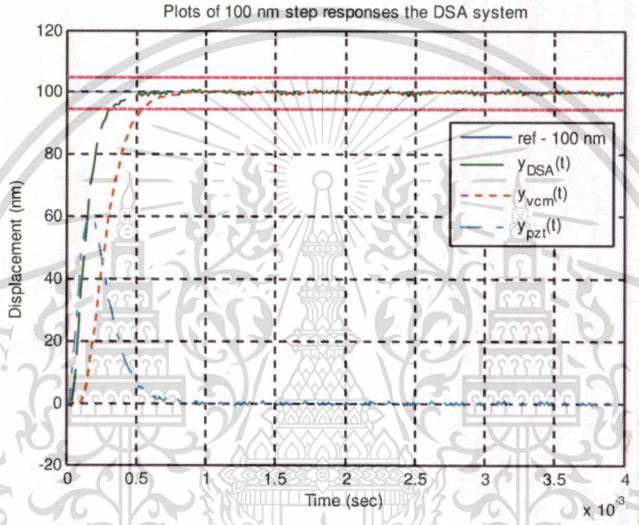

Fig. 4.9: Plots of 100 nm step responses the DSA track-following servo system.

The plots of the output states, internal states and following-error in comparisons between the VCM systems and the VCM reference model are illustrated in Fig. 4.10. The VCM controller states, switching surface and phase portrait of sliding motion are shown in Fig. 4.11. The control inputs (u) for the VCM actuator can be found in Fig. 4.12.

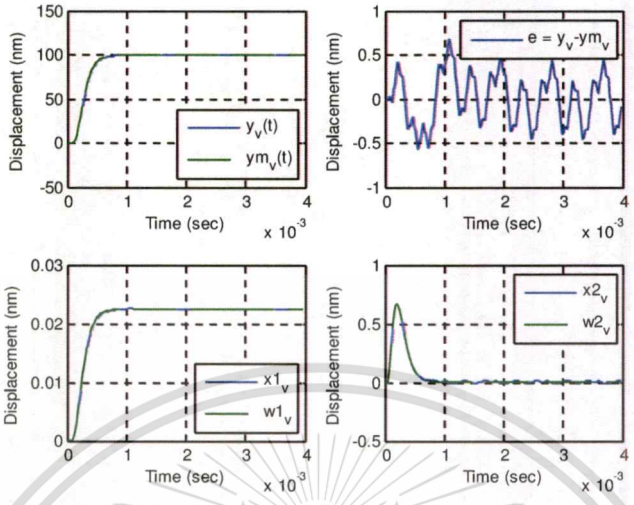

Fig. 4.10: Comparison plots of states between the VCM systems vs. VCM reference model.

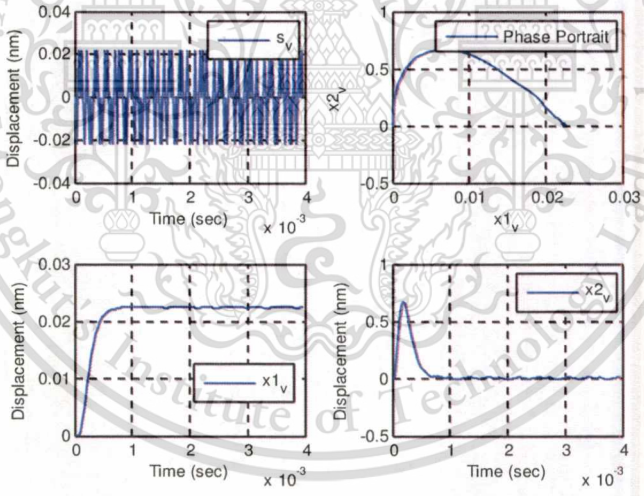

Fig. 4.11: Plots of switching surface and phase portrait of sliding motion of the VCM controller.

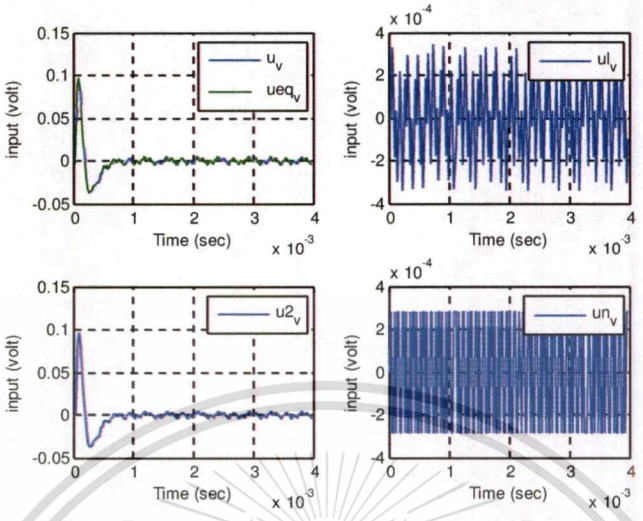

Fig. 4.12: Plots of input control effort for the VCM actuator.

The plots of the output states, internal states and following-error in comparisons between the PZT micro-actuator systems and the PZT reference model are illustrated in Fig. 4.13. The PZT controller states, switching surface and the phase portrait of sliding motion are shown in Fig. 4.14. The control inputs (u) for the PZT micro-actuator can be found in Fig. 4.15.

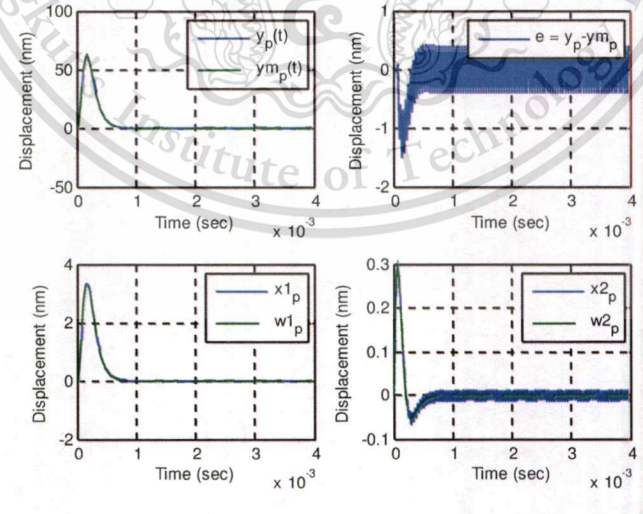

Fig. 4.13: Comparison plots of states between the PZT systems vs. PZT reference model.

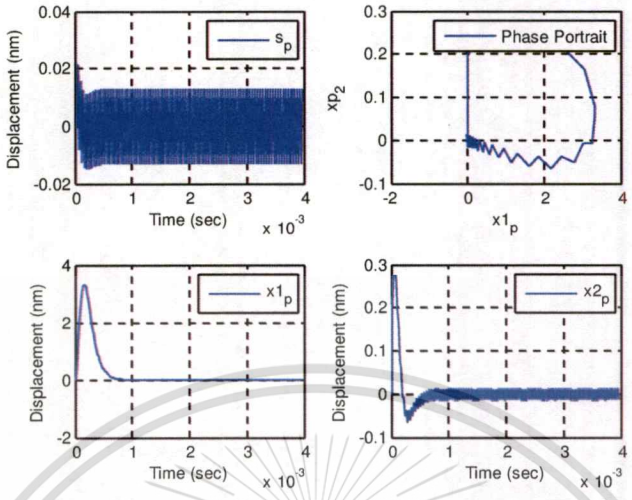

Fig. 4.14: Plots of switching surface and phase portrait of sliding motion of the PZT controller.

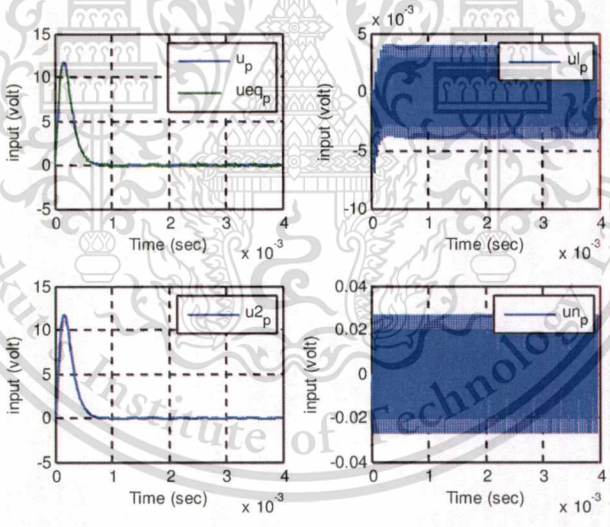

Fig. 4.15: Plots of input control effort for the PZT micro-actuator.

It can be seen that 100 nm step responses of the DSA track-following servo controller design using a model-reference SMC control are satisfied. The output of the system tracks the reference model properly. The following-error between the model output and the reference model are obtained less than 1 nm on the both actuators. It means that the system is robust against the disturbances. However, when control efforts

are considered, the switching control signals contribute the chattering which results in wear and tear of the actuators referred Fig. 4.15.

4.4 Chattering Reduction

The chattering occurs in the control systems is contributed from the term of u_n as referred to the control law in equation (3.54). It is equivalent to the signum function. We may consider of eliminating the u_n in order to reduce the chattering. The new control law is given by

$$\begin{aligned} u(t) &= Fx(t) + Gr(t) + Le(t) \\ F &= B^{\dagger}(A_m - A) \\ G &= B^{\dagger}B_m \\ L &= -(SB)^{-1}(SA_m - \Phi S) \end{aligned} \tag{4.3}$$

The step responses of 100 nm reference input command to the DSA system using the new control law for chattering reduction is illustrated in Fig. 4.16.

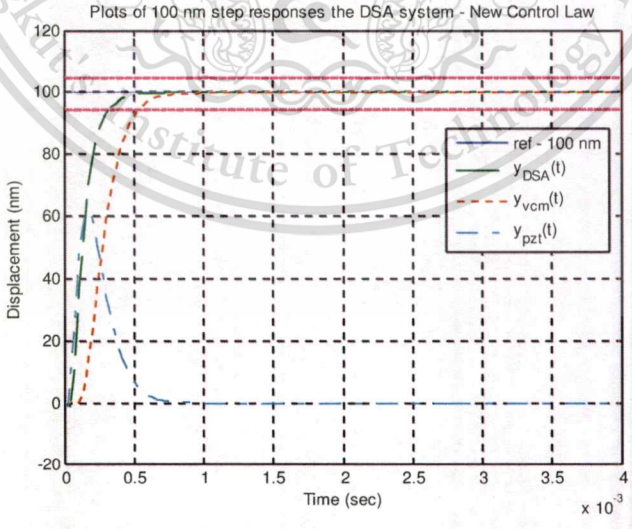

Fig. 4.16: Plots of 100 nm step responses the DSA new control law.

Using the new control law, the plots of states and following-error compared between the VCM systems and the VCM reference model are illustrated in Fig. 4.17. The controller states, switching surface and the phase portrait of sliding motion are shown in Fig. 4.18. The control inputs (u) for the VCM can be found in Fig. 4.19.

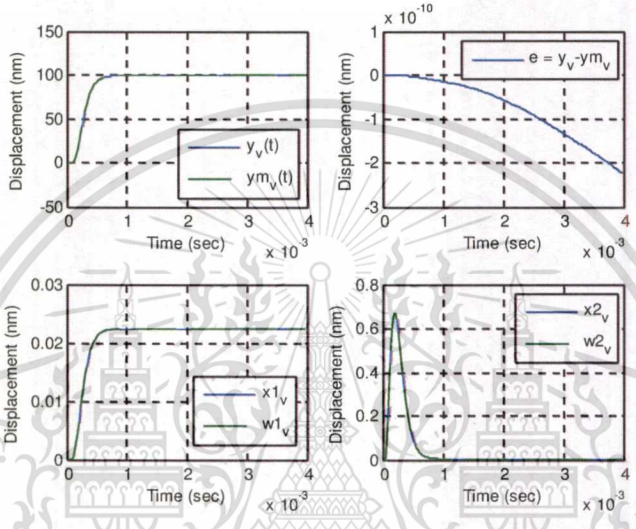

Fig. 4.17: Comparison plots of states between the VCM systems vs. VCM reference model.

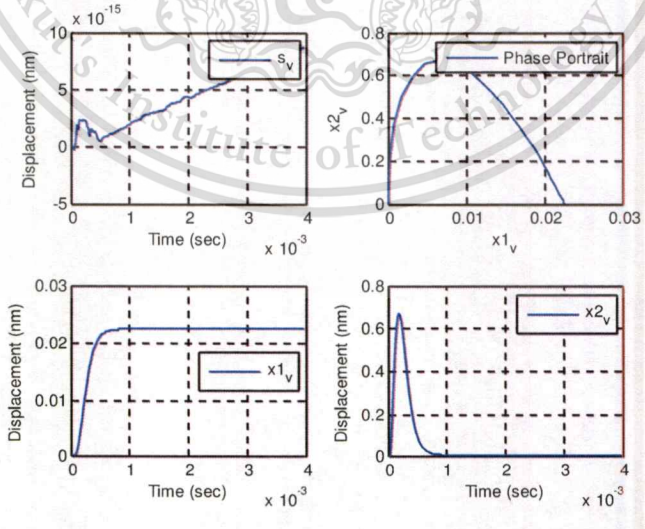

Fig. 4.18: Plots of switching surface and phase portrait of the VCM controller.

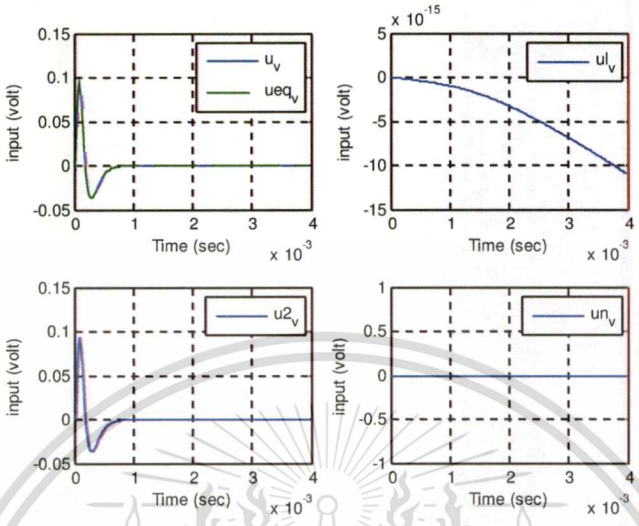

Fig. 4.19: Plots of input control effort for the VCM after reducing the chattering.

With the use of the new control law, the plots of system states compared between the PZT systems and the PZT reference model are illustrated in Fig. 4.20. The controller states, switching surface and the phase portrait of sliding motion are shown in Fig. 4.21. The control inputs (u) for the PZT micro-actuator can be found in Fig. 4.22.

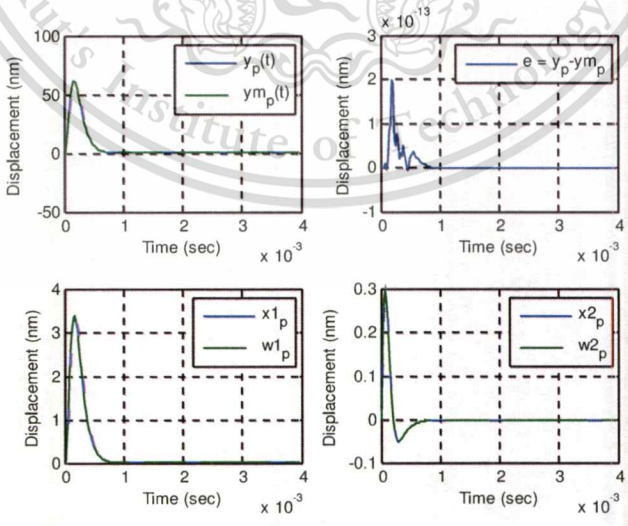

Fig. 4.20: Comparison plots of states between the PZT systems vs. PZT reference model.

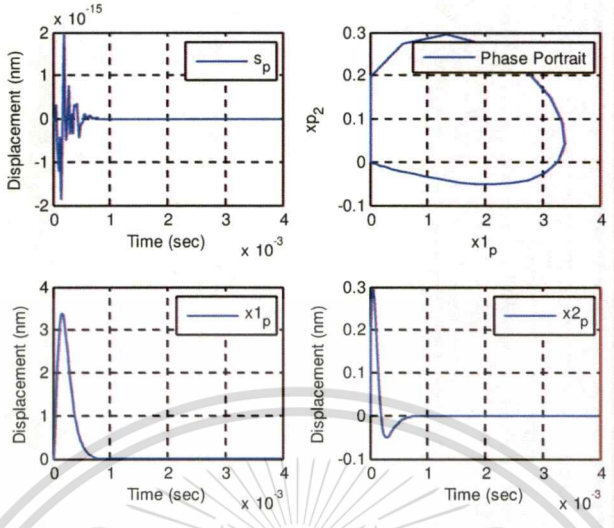

Fig. 4.21: Plots of switching surface and phase portrait of sliding motion of the PZT controller.

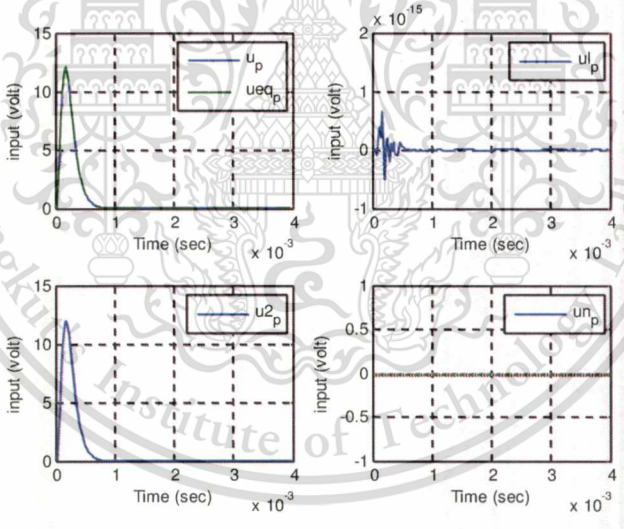

Fig. 4.22: Plots of input control effort for the PZT micro-actuator after reducing the chattering.

After the chattering elimination is implemented using by the new control law in equation (4.3), the significant reduction in the following-error between the system and the reference model could be obtained as well as the reduction of control effort to

both actuators. The control system performances such as rise-time, settling-time, and the overshoot remain the same.

The step response of the track-following servo controller design using a model-reference SMC in the DSA system is compared to the SSA system. The plots of 100 nm step response of the DSA compared to the SSA system are shown in Fig. 4.23.

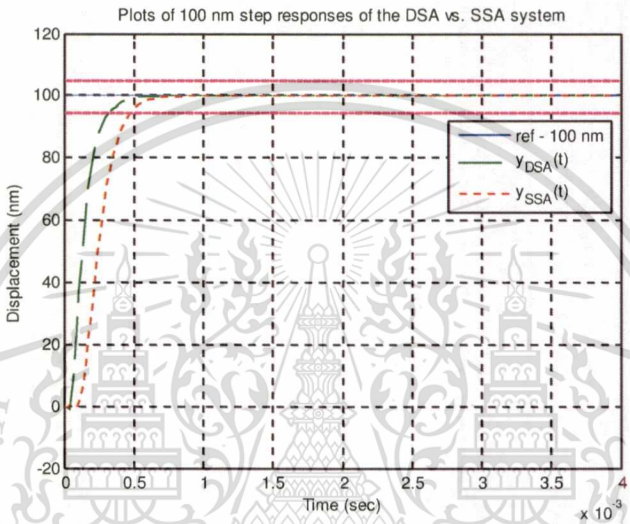

Fig. 4.23: Plots of 100 nm step responses the DSA compared to the SSA system.

The results show 30% reduction in the settling-time as the settling-time of the DSA is 0.35 msec. compared to the SSA at 0.5 msec. The overshoots of the displacement for both of the DSA and the SSA are less than 0.5% which met the requirement specifications. The performances comparisons are shown in Table 4.1.

Table 4.1 Performances Comparison Between DSA System vs. SSA System using a Model-Reference SMC Controller Design

Key Design Requirements	MRSMC Performance Results		
	Dual-Stage Actuator	Single-Stage Actuator	Difference (%)
Off-track rms (nm)	1.72 nm	2.79 nm	-
3δ of PES (nm)	5.16 nm	8.36 nm	-38.3%
Settling time (ms)	0.35 msec	0.5 msec	-30%
Rise time (ms)	0.2 msec	0.27 msec	-25.9%
Overshoot (%)	No overshoot	No overshoot	-

4.5 Benchmarking with PID

The performances of the track-following servo controller design using the model-reference SMC techniques in the DSA system are compared to the conventional technique using PID control. The ZieglerNichols PID tuning is used in this study, is given by

$$ZieglerC = \frac{k_p.t_i.t_d.(1+e_p).s^2 + k_p(t_i+e_p.t_d).s + k_p}{e_p.t_d.t_i.s^2 + t_i.s} \quad (4.4)$$

The filter is defined as e_p = 0.005 and tuning parameters k_{cr} and p_{cr} are obtained using the tools in Matlab software. The gain k_{cr} is the ultimate gain for closed-loop system until the output becomes oscillation, p_{cr} is the period of the oscillation frequency. The trial and error method is also applied for optimizing k_{cr} and p_{cr} to obtain better performance. In the VCM controller k_{cr} and p_{cr} are found as 0.02 and 0.04 respectively and k_{cr} = 50 and p_{cr} = 0.0001 are used for the PZT controller. The parameters obtained are referred to the classical Ziegler-Nichols tuning as $k_p = 0.6k_{cr}$, $t_i = 0.5p_{cr}$, and t_d =

$0.125p_{cr}$. Then the comparison plots of responses of the DSA track-following under present of the TMR are illustrated in Fig. 4.24.

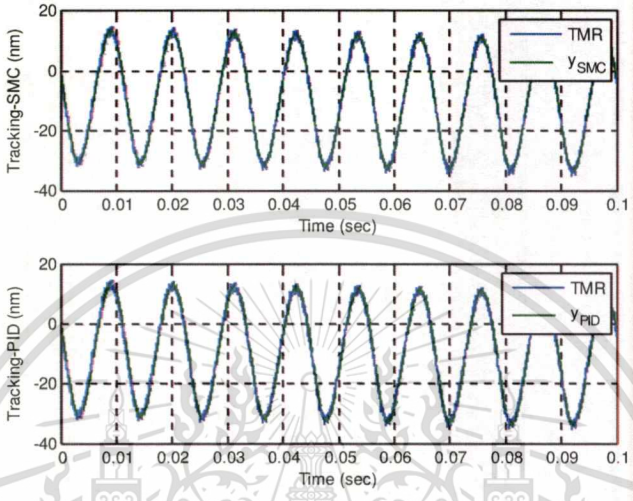

Fig. 4.24: Comparison of tracking performance using a model-reference SMC vs. PID.

The plots of tracking-error comparisons are shown in Fig. 4.25 and the 3σ PES positioning error tests are shown in Fig. 4.26.

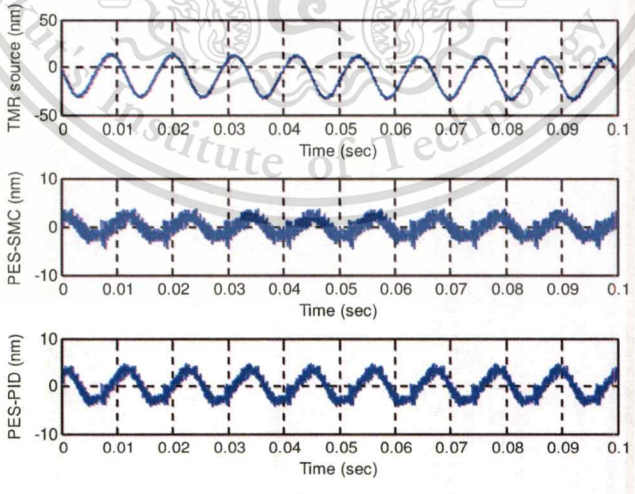

Fig. 4.25: Comparison of PES - tracking error using a model-reference SMC vs. PID.

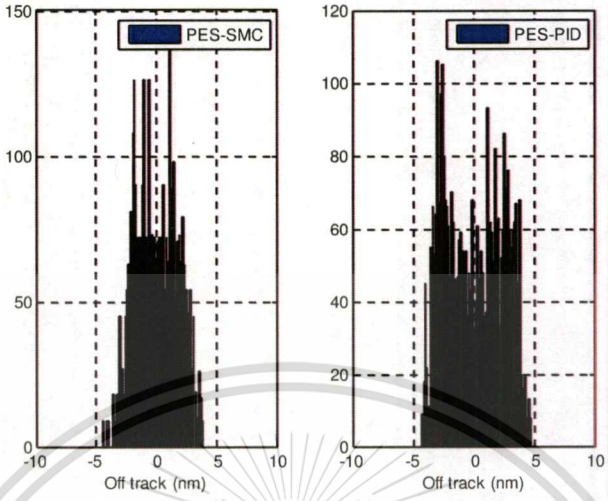

Fig. 4.26: Comparison of PES off-track (3σ) between a model-reference SMC vs. PID.

It is found that the 3σ PES off-track in the DSA system using proposed technique MRSMC is 5.16 nm, 28.03% better than the PID controller at 7.17 nm.

The comparison plots of 100 nm step responses of the DSA system between the proposed MRSMC and the classical PID design are shown in Fig. 4.27.

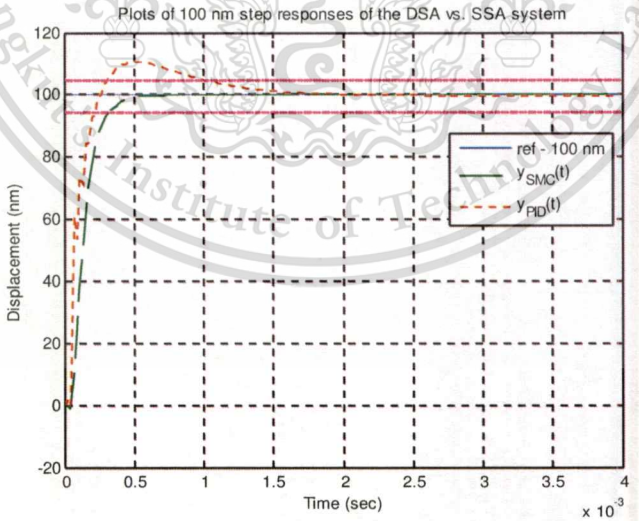

Fig. 4.27: Comparison plots of 100 nm step responses using MRSMC vs. PID.

The results show that no overshoot found in the proposed MRSMC design which is better when compared to the PID at 11.1% overshoot. The MRSMC controller also show better in the settling-time at 0.35 msec. compared to PID at 1 msec. The performances comparisons are shown in Table 4.2.

Table 4.2 Benchmarking a Model-Reference SMC Design vs. PID Control in the Dual-Stage Actuator Servo Control System

Key Design Requirements	The DSA Performance Results		
	MRSMC Control	PID Control	Difference (%)
Off-track rms (nm)	1.72 nm	2.39 nm	-
3δ of PES (nm)	5.16 nm	7.17 nm	-28.03%
Settling time (msec)	0.35 msec	1 msec	-65%
Rise time (msec)	0.2 msec	0.15 msec	25%
Overshoot (%)	No overshoot	11.1%	-11.1%

4.6 Discussions

The overall performances of the proposed technique using a model-reference SMC in DSA systems are discussed. The performances of proposed design are evaluated in the time-domain. The results show that the proposed MRSMC controller could be satisfied and met all requirements specifications. It is found that the model-reference SMC design is robust to the disturbances, as being proven by the PES (tracking error) testing as well as the ability of following the step input. The performances of the DSA system are compared to the SSA system. It is proven that the DSA system improves the servo performances. In addition, the performances of the proposed MRSMC controller in the DSA system could overcome the classical PID technique in the tracking performance benchmarking.

Chapter 5
Conclusion and Suggestion

The mathematical models of the VCM and PZT in dual-stage actuator system are obtained. The controller design for the dual-stage actuator system using in this study is based on the decouple scheme. The proposed control technique is developed with a model-reference based sliding mode control. The principle of this approach is that the plant system states are forced to follow the dynamics of an ideal model. If the control laws are properly designed then the perfect model-matching conditions guarantee that the system in the sliding model control is insensitive to the disturbances are discussed in Chapter 3. The simulation results are conducted and presented in Chapter 4 as well as the suggestion to eliminate the chattering in sliding mode. The proposed SMC design technique for the dual-stage actuator system is compared to the single-stage actuator. The benchmarking of the proposed SMC control with the classical PID control is also evaluated.

5.1 Conclusions

The main objective of this research is to develop a new approach of the track-following servo control for the dual-stage actuator in hard disk drive. This study is divided into two parts; the mathematical modeling of the dual-stage actuator and the design of model-reference sliding mode control (MRSMC) controller. In the model estimation, the least square fitting method is used with the help from Matlab tools. The VCM model estimation is obtained in a four-state model and the mathematical modeling of the PZT micro-actuator could be satisfied with a second-order model. The results of the model validation using random noises are acceptable in the loss functions and RMS errors compared with the true-models. A model-reference based sliding mode control approach is selected for the dual-stage actuator track-following servo control.

The controller design is based on the decouple scheme which enable the independent design procedures of the VCM and PZT.

There are three main steps of the controller design. For the first step, the reference models for the both actuators are designed using robust poles placement. It shows that the reference models could be satisfied in tracking error requirements without any overshoot or undershoot as well as rise-time and settling-time. The sliding surface for MRSMC is designed in the second step. The controller brings the trajectory onto the sliding surface and moves along the surface to the origin, meaning that controller has forced the error between the plant system and the reference model states to zero. This is to ensure that the plant system output follows the reference model output accordingly. The control laws are designed in the third step.

The simulations results are done in the time-domain. The performances of the controller design have been evaluated using the actual measured TMR sources obtained in drive operating. The settling-time and the overshoot are obtained from step response at 100 nm reference command. The 3σ PES for tracking error testing of the DSA is 5.16 nm which is 38.3% less when compared to the SSA system at 8.36 nm. The settling-time and rise-time were satisfied. The settling-time is 0.35 msec. which is 30.0% faster than the SSA at 0.5 msec. There is no overshoot found in both of the DSA and SSA using the MRSMC control.

The benchmark problem is also conducted in this study as the proposed design is compared to the classical PID control. The 3σ PES test of the MRSMC is 5.16 nm, 28.03% less than PID control at 7.17 nm. With the step response testing, there is 0.35 msec. which is 65% faster in the settling-time compared to the PID. No overshoot or undershoot observed with the proposed designed when compared to 11.1% overshoot found in the conventional PID technique.

The proposed MRSMC for the dual-stage actuator has been developed and proven that it can achieve all specification requirements. A MRSMC is robust against plant model uncertainty and disturbances. It is a superior controller achieving better tracking performance than the classical PID control, as shown by the simulation results. The chattering elimination shows the benefit of reducing wear and tear in the actuators,

while keeping the system on the sliding surface, resulting in less control efforts and would help improving the overall performances of the system. Then the method presented in this paper can also be applied to improve the performances of the dual-stage actuator even further.

5.2 Suggestions and Further Work

Although the MRSMC control method presented has been proven to be an acceptable tracking control strategy, there are some further improvements that could be done. This study only focused on the track-following servo control, the switching of the control mode between track-seeking and track-following was not considered in this study. It would be favorable to extend this controller design approach to cover the track-seeking as well. More work could be done in the future for control system improvement.

References

[1] Takashi Yamaguchi, "HDD Servo Control Development -Present and Future," SICE-ICASE International Joint Conference, October 2006

[2] K.C. Tan, et al., "Evolutionary design and implementation of a hard disk drive servo control system," Springer-Verlag, Published March 2006

[3] A. Al Mamun, T. H. Lee, and T. S. Low, "Frequency domain identification of transfer function model of a disk drive actuator," Mechatronics, vol. 12, pp. 563-574, May 2002.

[4] T. Suthasun, et al., "System identification and controller design for dual actuated hard disk drive," Control Engineering Practice 12 (2004)

[5] Bharat Bhushan (Ed.), Springer Handbook of Nanotechnology 2nd Edition. Springer 2005

[6] Chen BM, Lee TH, Venkataramanan V., Hard Disk Drives Servo Systems. Springer: New York, London, 2002

[7] Abdullah Al M., GuoXiao G, Chao Bi, Hard Disk Drive Mechatronics and Control. Taylor & Francis, 2007

[8] H. Numasato and M. Tomizuka, "Settling control and performance of a dual-actuator system for hard disk drives," IEEE-ASME Transactions on Mechatronics, vol. 8, pp. 431-438, Dec 2003.

[9] Kemao Peng, et al., "Design and implementation of a dual-stage actuated HDD servo system via composite nonlinear control," Mechatronics 14 (2004) 965–988

[10] Peter M. Young, et al., "Servo Control of a Dual-Stage Actuator for a High Performance Disk Drive, Part 1: Modeling and Simulation," IEEE, Proceedings of the American Control Conference Denver, Colorado June 4-6, 2003

[11] Peter M. Young, et al., "Servo Control of a Dual-Stage Actuator for a High Performance Disk Drive, Part 2: Controller Design and Implementation," IEEE, Proceedings of the American Control Conference Denver, Colorado June 4-6, 2003

[12] Steven J. Schroeck, et al., "On Compensator Design for Linear Time-Invariant Dual-Input Single-Output Systems," IEEE-ASME Transactions on Mechatronics, vol.6, No. 1, March 2001

[13] Jinchuan Zheng, et al., "Nonlinear Tracking Control for a Hard Disk Drive Dual-Stage Actuator System," 2007 IEEE International Conference on Control and Automation, Guangzhou, CHINA - May 30 to June 1, 2007

[14] V. Venkataramanan, et al., "A new approach to the design of mode switching control in hard disk drive servo systems," Elsevier Science, Control Engineering Practice 10 (2002) 925–939

[15] Roberto Horowitz, et al., "Dual-stage servo systems and vibration compensation in computer hard disk drive," Control Engineering Practice 15 (2007) 291–305

[16] Hongbo Zhang, et al., "Dual-stage HDD head positioning using an Hinf controller and a tracking differentiator," Mechatronics 19 (2009)

[17] Seung-Hi Lee, et al., "Design of A Dual-stage Actuator Control System with Discrete-Time Sliding Mode for Hard Disk Drives," IEEE Conference on Decision and Control, Australia, December 2000

[18] W.C. Wu, and T.S. Liu, "Sliding mode based learning control for track-following in HDD," Mechatronics 14 (2004)

[19] Tsang-Li Tai, Jian-Shiang Chen, "Discrete-time sliding-mode controller for dual-stage systems -A hierarchical approach," Mechatronics 15 (2005) 949–967

[20] G. Herrmann, et al., "Application of a discrete sliding mode technique to a HDD dual-stage track-seek and track-following servo system," 22nd IEEE International Symposium on Intelligent Control (2007)

[21] Qinglei Hu, et al., "Discrete-Time Sliding Mode Control With Time-Varying Surface for Hard Disk Drives," IEEE Trans Control System Technology, Vol. 17, January 2009

[22] Edwards C, Spurgeon SK, Sliding Mode Control: Theory and Applications. Taylor & Francis: U.K., 1998.

[23] Utkin, V. I., Sliding Modes in Control Optimization, Springer-Verlag, Berlin, 1992.

[24] Khalil, H. K., Nonlinear Systems, Prentice Hall, 2001.

Biography

Full Name	Mr. SIWAPHON SONKHAM
Date of Birth	April 1979
Birth Place	Nakhon Si Thammarat
Resident	Passorn2 Village, M. 3, T. Klong.3, Klongluang, Pathumthani, Thailand
Email:	tunergear@gmail.com
Education	- Diploma Degree in Electrical Electronics, 1997-1999 Rajamangala Institute of Technology North Bangkok, Thailand - B.Eng. in Electronics Engineering, 1999-2002 King Mongkut's Institute of Technology Ladkrabang, Thailand
Work Experiences	
2006 - Present	Western Digital Thailand, Bang pa-in, Ayutthaya, Thailand
2002 - 2006	Celestica Thailand, Laem Chabang, Chonburi, Thailand
Publication	- Patent US 8322235 B1, "Microactuator test assembly comprising a spreader pin for engaging a load beam of an actuator arm", Assigned to Western Digital Technologies, Inc., 2012 - ICCSSP 2014, International Conference on Circuits, Systems, and Signal Processing, "A Model-Reference Sliding Mode for Dual-Stage Actuator Servo Control in Hard Disk Drive", Singapore, March 2014 - ECTI-CON 2014 : The 2014 International Conference on Electrical Engineering/Electronics, Computer, Telecommunications and Information Technology, "A Model-Reference Sliding Mode Control for Dual-Stage Actuator in Hard Disk Drive", Thailand, May 2014
Special Interest	- PZT Failure Characteristics and Detections - PZT Micro-Actuator Testing in Hard Disk Drive Manufacturing - Dual-Stage Actuator Servo Control in Hard Disk Drive

Publication

ECTI-CON 2014 : The 2014 International Conference on Electrical Engineering/Electronics, Computer, Telecommunications and Information Technology, "A Model-Reference Sliding Mode Control for Dual-Stage Actuator in Hard Disk Drive", Thailand, May 2014

A Model-Reference Sliding Mode for Dual-Stage Actuator Servo Control in HDD

Siwaphon Sonkham
College of Data Storage and Innovation, King Mongkut's Institute of Technology Ladkrabang, Bangkok, Thailand
tunergear@gmail.com

Unnat Pinsopon
Faculty of Engineering, King Mongkut's Institute of Technology Ladkrabang, Bangkok, Thailand
kpunnat@kmitl.ac.th

Withit Chatlatanagulchai
Data Storage Technology Research Unit, Kasetsart University, Bangkok, Thailand
fengwtc@ku.ac.th

***Abstract*—This paper presents a method of sliding mode control (SMC) designing and developing for the servo system in a dual-stage actuator (DSA) hard disk drive. Mathematical model of hard disk drive actuators is obtained, extracted from measuring frequency response of the voice-coil motor (VCM) and micro-actuator separately. The Matlab software tools are used for mathematical model estimation and also for controller design and simulation. A model-reference approach for tracking requirement is selected as a proposed technique. The simulation results show that performance of the model-reference SMC controller in DSA servo control can be satisfied in the tracking error, as well as keeping the positioning of the head within the boundary of +/-5% of track width under the presence of disturbance. The overall results of model-reference SMC design in DSA are met per requirement specifications and significant reduction in %off track is found when compared to the single-state actuator (SSA).**

Keywords—Hard Disk Drive, Dual-Stage Actuator, Track Following, HDD Servo Control, Sliding Mode Control, Model-Reference, Tracking Control

I. INTRODUCTION

In Hard Disk Drive (HDD) industry, capacity and access performance are major product specifications. To achieve larger capacity, increasing areal density is most important. In order to increase areal density in an HDD, a servo system is one of the most significantly factors that need to be improved with high accuracy to achieve the principle requirements. The accuracy of read/write (R/W) head positioning on the center of a target track is a key factors which requires a positioning in the order of a few nanometers. In order to develop high bandwidth track-following servo systems, DSA in the HDD has been proposed as an effective solution to overcome the limitation. DSA has been involved and developed by integrating the piezoelectric materials for acting as a secondary actuator in order to keep the R/W head on the desired track accurately. The suspension-based DSA is being introduced for use in HDDs, by integrating PZT (lead-zirconate-titanate) material placed onto the suspension of head-gimbal assembly (HGA) located between slider R/W head and HGA base plate. In DSA servo systems, the VCM is actuated as the primary stage to provide long track seeking but with poor accuracy and slow response time, while the PZT is used as a secondary actuator to provide higher precision and faster response but has limitation in stroke. When combining them with properly designed controllers, both actuators are complementary to each other. The implementation of the HDD servo controller relies on the positioning error signal (PES), which is obtained by reading the position information encoded on the disk's data tracks. The position error is also called track mis-registration (TMR) in the HDD industry. Major TMR sources in the track-following mode includes spindle run out, disk fluttering, bias force, external vibration/shock disturbance, vibrations due to air turbulence, and PES noise. [1]-[5]

Various control designs have been developed for DSA control and can be largely classified into two categories as: the first group based on decoupled or sequential single-input single-output (SISO) designs, and the other group based on modern optimal design methodologies.[6],[7]. In existing literature, either adaptive or robust control algorithms or both were designed to handle external disturbance and model uncertainties. Hidehiko and Masayoshi [8] presented a settling control of a DSA for HDD; the decoupling filter (PZT output estimator) is canceled at the VCM controller input. Peng, et al. [9] presented that the DSA can increase the control bandwidth for track-following performance based on a composite nonlinear control. Zheng and Tomizuka [10] proposed an adaptive compensation scheme to estimate and compensate the non-repeatable run out. You and Hong [11] proposed a robust SMC with a new switching surface for track-following. Low and Wong [12] used a multi-objective genetic algorithm in a controller-tuning scheme for a HDD servo by priority at constraint objectives rather than the optimization. Taghirad and Jamei [13] applied an adaptive robust control. Du et al. [14] devised a linear controller based on solving linear matrix inequalities for actuator positioning using an adaptive nonlinear compensation. Horowitz, et al. [15] studied the vibration compensation for disturbance rejection in DSA. Zhang, et al. [16] used an Hinf for DSA head positioning and a tracking control. The SMC approach has been found for DSA control in HDD. Lee, et al. [17] studied discrete-time design of a DSA control using a state estimator based SMC in the discrete time domain. Wu, et al. [18] developed SMC based learning for track-following in HDD; the learning algorithm utilizes shape functions and estimate the control input to reduce repetitive error. Tsang-Li Tai and Jian-Shiang Chen [19] designed SMC for tracking performances for large and fine range; the settling-time could be found by selecting a sliding hyper-plane.

Herrmann, et al. [20] studied SMC combined into the observer-based for micro-actuator; the design state feedback controller used an LQR approach for the discrete-time SMC. Hu, et al. [21] adopt an approximate time optimal switching for the time-varying SMC, resulting in smooth transition for both track seeking and following.

This paper presents the design of SMC for DSA track following servo control in the HDD. The SMC used in this paper is based on the model-reference approach, suitable for tracking of multi-input-multi-output (MIMO) systems, was taken from [22]. The SMC has been studied and proven that it has attributed to robustness for dealing with the parametric uncertainties and disturbances. Basics of the SMC method can be found from [22]-[24] and references therein. DSA plant transfer functions have been obtained by fitting a model from its measuring data that has been extracted by exciting the actuators with the swept frequency sinusoidal input signal. The magnitude and phase from its frequency response data are used in order to obtain an estimated model, and then the proposed design of servo control is developed. Matlab software is used for model estimation, controller design, simulation and evaluation to observe the performance. The organization of this paper is as follows: A description of obtaining the mathematic modeling of dual-stage actuators is provided in Section II. The principles of sliding mode and controller design are given in Section III. Results of this study are shown and discussed in Section IV. Section V. presents conclusions and summarizes the outcome of this work.

II. DUAL STAGE ACTUATOR MODEL

Normally, the DSA consists of two actuators: the first is the VCM and the second actuator is the PZT so called micro-actuator, which is mounted on the active suspension located between the R/W head slider and the HGA base plate. Fig.1 illustrates the DSA used in designing our control system. u_v and u_p are the voltage inputs and y_v and y_p are the linear displacements of the VCM and PZT respectively.

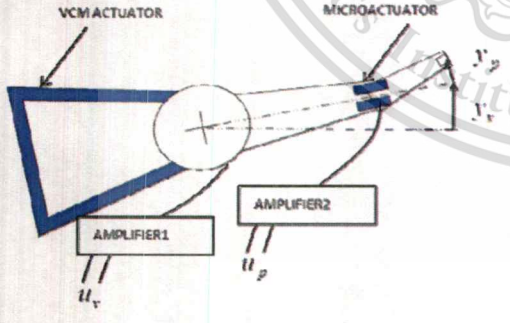

Fig. 1. Schematic of Dual-Stage Actuator in HDD.

The frequency response of the VCM and PZT are measured from displacement of the head when injecting the sweep sine source at the frequency range of drive operation. Normally, the frequency response of the both actuators can be represented by a rigid model G_{rigid} with their several resonance modes ***Res*** as shown in equation (1) and (2) respectively.

$$G_{rigid} \approx \frac{K\omega_p^2}{S^2+2\zeta\omega_p S+\omega_p^2} \tag{1}$$

$$\mathrm{Re}\,s \approx \prod_{i=1}^{n} \frac{S^2+2\zeta_{zi}\omega_{zi}S+\omega_{zi}^2}{S^2+2\zeta_{pi}\omega_{pi}S+\omega_{pi}^2} \tag{2}$$

The model estimation can be obtained by using tools in Matlab software. The comparison plot of frequency response of VCM is shown in Fig.2 and the response plot of PZT is illustrated in Fig.3.

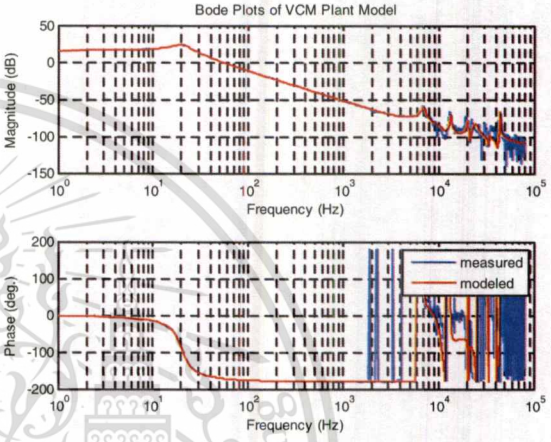

Fig. 2. Comparison of VCM actual and VCM model estimation.

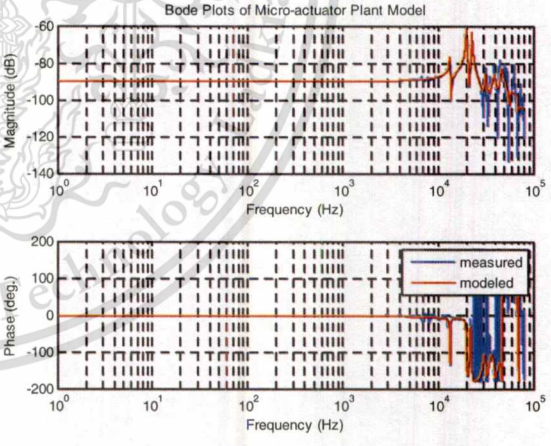

Fig. 3. Comparison of PZT actual plant and PZT model estimation.

The state-space model of the second-order rigid model in the LTI system can be obtained in form as below:

$$\begin{aligned} x(t)' &= Ax(t)+Bu(t) \\ y(t) &= Cx(t) \end{aligned} \tag{3}$$

where $A \in \mathbb{R}^{nxn}$, $B \in \mathbb{R}^{nxm}$ and $C \in \mathbb{R}^{pxn}$, $1 \le m < n$. The variables x is a vector of state variables, y is a vector of plant outputs, and u is a vector of control. If the rank (B) = m and the pair (A, B) is controllable, the plant model can be transformed into regular form as

$$\begin{bmatrix} x_1' \\ x_2' \end{bmatrix} = \begin{bmatrix} A_{11} & A_{12} \\ A_{21} & A_{22} \end{bmatrix} \begin{bmatrix} x_1 \\ x_2 \end{bmatrix} + \begin{bmatrix} 0 \\ B_2 \end{bmatrix} u \qquad (4)$$
$$y = \begin{bmatrix} C_1 & C_2 \end{bmatrix} x$$

where $x_1 \in \mathbb{R}^{n-m}$, $x_2 \in \mathbb{R}^{m}$, A_{11}, A_{12}, A_{21}, A_{22}, B_2, C_1, and C_2 are constant matrices with corresponding dimensions. We consider in state-space form so the second-order of the VCM rigid model can be written as below.

$$\begin{bmatrix} x_1' \\ x_2' \end{bmatrix} = \begin{bmatrix} -11.55 & 125.3 \\ -125.3 & -11.55 \end{bmatrix} x + \begin{bmatrix} 0 \\ 36.01 \end{bmatrix} u_v \qquad (5)$$
$$y_v = \begin{bmatrix} 23.52 & -0.0979 \end{bmatrix} x$$

And then the second-order state-space form of the PZT model can be found as.

$$\begin{bmatrix} x_1' \\ x_2' \end{bmatrix} = \begin{bmatrix} -3.167\text{x}10^3 & 1.323\text{x}10^5 \\ -1.323\text{x}10^5 & -3.167\text{x}10^3 \end{bmatrix} x + \begin{bmatrix} 0 \\ 1.487 \end{bmatrix} u_p \qquad (6)$$
$$y_p = \begin{bmatrix} 1.146 & -0.2601 \end{bmatrix} x$$

III. Model Reference SMC Design

A. Model-References

The sliding mode control is one of the robust controller designs for nonlinear dynamic plants operating under uncertain conditions. The main advantage of the SMC is low sensitivity of plant parameter variations, model uncertainties and disturbances. Usually, SMC is considered a high-speed switching feedback control because of the variable structure control type. The purpose of the switching control law is to drive the plant state trajectory onto a predetermined surface in the state-space and then to maintain the state trajectory on that surface. This surface is called the "sliding surface". The state variables are driven to a sliding surface and maintained there; this process is called "reaching phase". Once trajectory is intercepted at the sliding surface, the switching control maintains the plant state trajectory on the surface and the state variables on the sliding surface move to the origin, called "sliding phase". As a result, the closed-loop system dynamics are determined by the plant state trajectory restricted to the sliding surface. In the model-reference SMC, a reference model is relating to the plant output. The SMC controller is designed, so that the errors between the reference model state variables and the plant state variables are driven to zeros. Resulting in the plant output is close to the reference model output, and then the specifications can be met. We consider the reference model as

$$w(t)' = A_m w(t) + B_m r(t)$$
$$y_m(t) = C_m w(t) \qquad (7)$$

where $A_m \in \mathbb{R}^{nxn}$, $B_m \in \mathbb{R}^{nxm}$ and $C_m \in \mathbb{R}^{pxn}$, $1 \le m < n$, so the variables w is a vector of state variables, y_m is a vector of reference model outputs, and r is a vector of reference inputs. If the rank (B_m) = m and the pair (A_m, B_m) is controllable, the reference model can be transformed into regular form as

$$\begin{bmatrix} w_1' \\ w_2' \end{bmatrix} = \begin{bmatrix} A_{m11} & A_{m12} \\ A_{m21} & A_{m22} \end{bmatrix} \begin{bmatrix} w_1 \\ w_2 \end{bmatrix} + \begin{bmatrix} 0 \\ B_{m2} \end{bmatrix} r \qquad (8)$$
$$y_m = \begin{bmatrix} C_{m1} & C_{m2} \end{bmatrix} w$$

where $W_1 \in \mathbb{R}^{n-m}$, $W_2 \in \mathbb{R}^{m}$, A_{m11}, A_{m12}, A_{m21}, A_{m22}, B_{m2}, C_{m1}, and C_{m2} are constant matrices with corresponding dimensions. The reference model (A_m, B_m) can be formulated so that the model outputs y_m follow the reference inputs r with desirable transient response. One way to find the matrices A_m and B_m is to use pole-placement method. If we want to design u for the plant model (3) to have desirable closed-loop poles and to ensure steady-state tracking is zero, we choose

$$u = Fx + Gr \qquad (9)$$

Then, the closed-loop system becomes $x' = (A + BF)x + BGr$, $y = Cx$ and the transfer function from r to y is given by

$$\frac{y(s)}{r(s)} = C\left(sI - \left(A + BF\right)\right)^{-1} BG$$
$$G = -\left(C\left(A + BF\right)^{-1} B\right)^{-1} \qquad (10)$$

A full-state feedback matrix F can be designed to place the closed-loop poles at desired locations to achieve desirable transient response. To ensure steady-state tracking of a step reference, using the final-value theorem. Therefore, the reference model can be chosen as $A_m = A + BF$ and $B_m = BG$. The reference models for both actuators are found by placing the poles of (A, B). The poles at [$-5\text{x}10^3$, $-6\text{x}10^3$] are placed for VCM, then the closed-loop reference model can be found as

$$\begin{bmatrix} w_{m1}' \\ w_{m2}' \end{bmatrix} = \begin{bmatrix} -11.55 & 125.3 \\ -2.384\text{x}10^5 & -1.099\text{x}10^4 \end{bmatrix} w_v + \begin{bmatrix} 0 \\ 1.018\text{x}10^4 \end{bmatrix} r_v$$
$$y_{mv} = \begin{bmatrix} 23.52 & -0.0979 \end{bmatrix} w_v$$

and the poles [-5x10^3, -1x10^4] are placed to get the reference model of PZT as below.

$$\begin{bmatrix} w_{m1}' \\ w_{m2}' \end{bmatrix} = \begin{bmatrix} -3.167\text{x}10^3 & 1.323\text{x}10^5 \\ -94.64 & -1.183\text{x}10^4 \end{bmatrix} w_p + \begin{bmatrix} 0 \\ 331.6 \end{bmatrix} r_p$$

$$y_{mp} = \begin{bmatrix} 1.146 & -0.2601 \end{bmatrix} w_p$$

B. Model-Reference Sliding Mode Control

The whole design of an SMC system is to properly choose or design a sliding surface, that the closed-loop system has desired dynamics. And then a switching control that can drive the plant state trajectory onto the sliding surface and maintain it on that surface is to be designed. The control inputs u will make x tracks w, corresponding to y tracks y_m. Let $e = x - w$ be the error between the plant state variables and the reference model state variables. From (3) and (7), the error dynamics are given by

$$e' = A_m e + (A - A_m)x + Bu - B_m r \tag{11}$$

Consider a control law

$$u = u_l + u_n + u_2 = v + u_2 \tag{12}$$

where;

$$u_2 = B^{\dagger}(A_m - A)x + B^{\dagger}B_m r \tag{13}$$

u_2 is an inverse dynamics term with $B^{\dagger}$ as pseudo-inverse of B. Substituting (12) into (11), we have $e' = A_m e + Bv$. Since both plant model and reference model are in regular form, the error dynamics can also be written in regular form as

$$\begin{aligned} e_1' &= A_{m11}e_1 + A_{m12}e_2 \\ e_2' &= A_{m21}e_1 + A_{m22}e_2 + B_2 v \end{aligned} \tag{14}$$

Let the switching surface be

$$s = Se = S_1 e_1 + S_2 e_2 = S_2 M e_1 + S_2 e_2 \tag{15}$$

where S, S_1, S_2, and M are constant matrices with appropriate dimensions. S_2B_2 is any nonsingular diagonal matrix, normally chosen to be B_2 so that $S_2 = I$. Using a linear change of coordinates

$$T_s \overset{\Delta}{=} \begin{bmatrix} \mathrm{I} & 0 \\ \mathrm{S}_1 & \mathrm{S}_2 \end{bmatrix}, \text{ we have } \begin{bmatrix} e_1 \\ s \end{bmatrix} = T_s \begin{bmatrix} e_1 \\ e_2 \end{bmatrix}$$

Choose

$$u_l = -(SB)^{-1}(SA_m - \Phi S)e \tag{16}$$

where Φ is any stable design matrix, and then choose

$$u_n = -\rho(SB)^{-1}\frac{P_2 s}{\|P_2 s\|} \tag{17}$$

where $\rho > 0$ is a design parameter and P_2 is a symmetric positive definite matrix equation

$$P_2\Phi + \Phi^T P_2 = -I$$

After a straight-forward derivation, we obtained

$$e_1' = (A_{m11}e_1 - A_{m12}M)e_1 + (A_{m12}S_2^{-1})s$$

$$s' = \Phi s - \rho\frac{P_2 s}{\|P_2 s\|}$$

Consider a Lyapunov function $V_1 = s^T P_2 s > 0$, so the derivative is given by

$$\begin{aligned} V_1' &= s^T{}' P_2 s + s^T P_2 s' \\ &\le \|s\|^2 - 2\rho\|P_2 s\| \\ &\le -2\rho\sqrt{\lambda_{\min} P_2}\sqrt{V_1} \\ &\le 0 \end{aligned}$$

From the Rayleigh principle, we can conclude that s will approach zeros in finite time and will remain there afterward. Consider another Lyapunov function $V_2 = e_1^T P_1 e_1 > 0$, where P_1 is a unique symmetric positive definite solution to the Lyapunov equation

$$P_1(A_{m11} - A_{m12}M) + (A_{m11} - A_{m12}M)^T P_1 = -Q_1,$$

where; $Q1$ is a design symmetric positive definite matrix and M to be obtained and $(A_{m11} - A_{m12}M)$ is a stable matrix. So that we can conclude that e_1 will approach zeros in finite time and will remain there afterward, and during time $s = 0$, the result in e_2 will also approach zeros.

The advantages of SMC on this approach are as follows:

- Plant model is normally not required. However, knowing the plant model helps improve the quality of the control system, such as utilizing plant models to compute a controller parameters rather than by trial-and-error, and can be feed-forwarded to cancel known terms results in reducing the effort from fast-switching.

- During the sliding phase, the system order reduces from n to $n-m$, where n is the number of state variables and m is the number of inputs, making low complexity.
- During the sliding phase, the system is not affected by matched uncertainties, such as disturbances, noises, and plant uncertainties that can be directly altered by the control inputs.

C. Controller Design

In this study, the block diagram of the overall control system of DSA is designed as shown in Fig.4. This is based on the requirements that the micro-actuator must settle down to zero before its next move. During operation, only the total head displacement $y = y_v + y_p$ is measured. While the displacements for the feedback control system y_v and y_p were only estimated based on the fact that the micro-actuator can be accurately approximated by a constant gain, under the present range of operating frequency. The objective of SMC designs is to have the displacement of the head tracks a reference input when the following specifications are met:

- The mean of the steady-state error is zero.
- The 3σ PES is to be less than 10% of track width under desired TMR disturbance.
- The 5% settling time of step response is to be short as short as possible and overshoot is less than 5%.

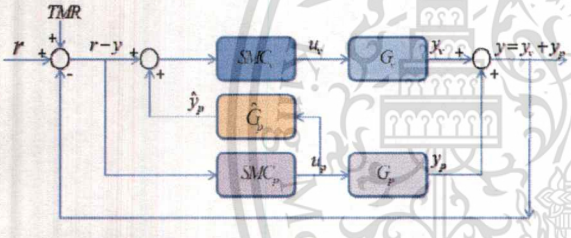

Fig. 4. Schematic diagram of dual-stage actuator control.

The DSA control loop from r to y consists of G_v is VCM plant that can be considered in a series with desired notch filter for system stabilizing. SMC_v is a controller designed for VCM plant. G_p is plant of PZT that can also be considered to connect in a series with notch filter to improve stability of the PZT plant and system. SMC_p is controller designed of PZT plant. Final block is $\hat{G}_p$ decoupling, estimated as a constant gain. $\hat{G}_p$ is placed between the VCM controller input and the PZT controller output. Then, $\hat{y}_p \cong y_p = y - y_v$, so that the PZT actuator output is canceled at the VCM controller input. The r is representing the input commands for DSA servo control to move the head and position onto the target track. Let $r - y$ is to be the controller input of micro-actuator. In the track-following task servo control, r is replaced by TMR to be the input to the controller. Normally, TMR consists of repeatable run out (RRO), non-repeatable run out (NRRO) and external disturbances. Considering the controller parameters, choose M to place the poles of ($A11$, $A12$) at [-10, -20] and P_2 to be I_m, so that S for both actuators will be found as.

$$S_v = [0.0123 \quad -1], \text{ and } S_p = [0.0238 \quad -1],$$

then Φ can be obtained by solving the Lyapunov function in Matlab, and normally set $\rho = 1$. The simulation results can be discussed in following section.

IV. Simulation Results

In the simulation results of the proposed technique, model-reference SMC for DSA track-following servo control could be satisfied and met all of the specifications. In track-following, the main objective is to achieve the TMR disturbance rejection. The TMR source for this evaluation is referring from [6].

$$r_{TMR}(t) = 0.5 + 0.1\cos(110\pi t) + 0.05\sin(220\pi t) + 0.02\sin(440\pi t) + 0.01\sin(880\pi t)$$

The results of tracking error comparing between DSA and SSA are shown in Fig.5, and the 3σ of %off track PES testing are obtained in Fig.6. The performance values are compared in Table 1.

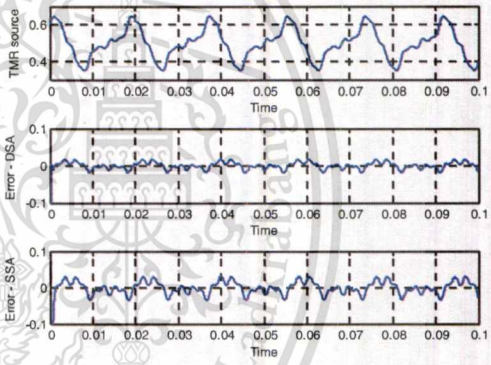

Fig. 5. Comparison of TMR disturbance rejection using model-reference SMC between DSA(dual-stage) and SSA(single-stage).

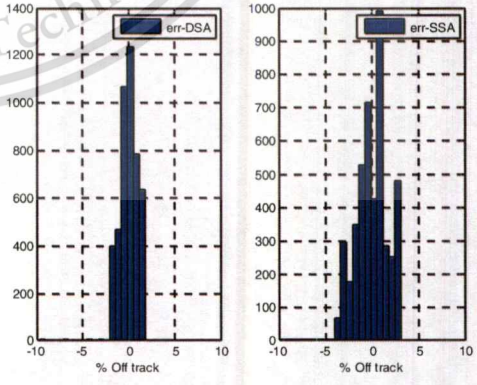

Fig. 6. Comparison of %off track (PES) using model-reference SMC between DSA(dual-stage) and SSA(single-stage).

The step responses of DSA with proposed model-reference SMC controller design is illustrated in Fig.7. Results show the 5% settling-time is 0.35 msec. compared to SSA at 0.63 msec. and the overshoot of the head displacement is less than 5% which are met per requirement specifications.

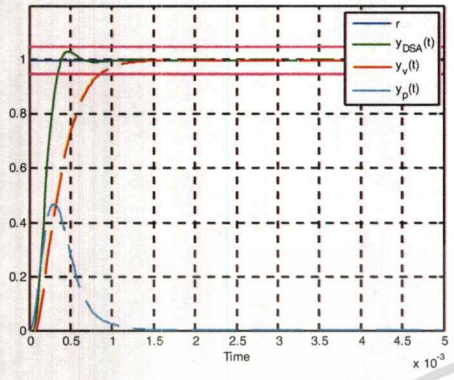

Fig. 7. Plot of response head displacement, VCM displacement and PZT displacement on DSA with model-reference SMC.

TABLE I. PERFORMANCES COMPARISON

Item	Time-Domain Performances Comparison		
	Performance Criteria	*Dual-Stage Actuator*	*Single-stage Actuator*
1	3δ of PES (%off track)	2.79	5.23
2	Settling time (ms)	0.35	0.63
3	Over shoot (%)	3.11	4.12

V. CONCLUSION

In this paper model-reference SMC has provided robustness against plant model uncertainty and disturbances. The reference model is relating reference to the plant output, is formulated to meet various time-domain specifications. The SMC controller is designed and shown that the errors between the reference model state variables and the plant state variables are driven to zeros. As a result, the plant output is closed to the reference model output, and the specifications can be met. The performance of proposed controller has been verified through Matlab simulation and can be proven that the DSA servo control was a superior controller when compare to SSA. The method presented in this paper can also be applied to improve the performance of the dual-stage actuator even further.

ACKNOWLEDGMENT

The authors would like to thank Western Digital (Thailand) Co., Ltd. for providing some technical assistance and financial support to complete this research.

REFERENCES

[1] Takashi Yamaguchi, "HDD Servo Control Development -Present and Future," SICE-ICASE International Joint Conference, October 2006

[2] K.C. Tan, et al., "Evolutionary design and implementation of a hard disk drive servo control system," Springer-Verlag, Published March 2006

[3] A. Al Mamun, T. H. Lee, and T. S. Low, "Frequency domain identification of transfer function model of a disk drive actuator," Mechatronics, vol. 12, pp. 563-574, May 2002.

[4] T. Suthasun, et al., "System identification and controller design for dual actuated hard disk drive," Control Engineering Practice 12 (2004)

[5] Bharat Bhushan (Ed.), Springer Handbook of Nanotechnology 2nd Edition. Springer 2005

[6] Chen BM, Lee TH, Venkataramanan V., Hard Disk Drives Servo Systems. Springer: New York, London, 2002

[7] Abdullah Al M., GuoXiao G, Chao Bi, Hard Disk Drive Mechatronics and Control. Taylor & Francis, 2007

[8] H. Numasato and M. Tomizuka, "Settling control and performance of a dual-actuator system for hard disk drives," IEEE-ASME Transactions on Mechatronics, vol. 8, pp. 431-438, Dec 2003.

[9] Kemao Peng, et al., "Design and implementation of a dual-stage actuated HDD servo system via composite nonlinear control," Mechatronics 14 (2004) 965–988

[10] Zheng, Q. and M. Tomizuka., "Compensation of Dominant Frequency Components of Nonrepeatable Disturbance in Hard Disk Drives," IEEE Transactions on Magnetics. Vol. 43. No. 9. pp. 3756-3762. 2007

[11] You, K.H. and M. Hong, "Robust Linear Quadratic Sliding-Mode Control for Hard Disk Drives," IEEE Transactions on Instrumentation and Measurement. Vol. 56. No. 3. pp. 1087-1093. 2007

[12] Low, K.S. and T.S. Wong., "A Multiobjective Genetic Algorithm for Optimizing the Performance of Hard Disk Drive Motion Control System," IEEE Transactions on Industrial Electronics. Vol. 54. 2007

[13] Taghirad, H.D. and E. Jamei., "Robust Performance Verification of Adaptive Robust Controller for Hard Disk Drives," IEEE Transactions on Industrial Electronics. Vol. 55. No. 1. pp. 448-456. 2008.

[14] Du, C., et al., "Disturbance Rejection for a Data Storage System via Sensitivity Loop Shaping and Adaptive Nonlinear Compensation," IEEE/ASME Transactions on Mechatronics. Vol. 13. No. 5. 2008

[15] Roberto Horowitz, et al., "Dual-stage servo systems and vibration compensation in computer hard disk drive," Control Engineering Practice 15 (2007) 291–305

[16] Hongbo Zhang, et al., "Dual-stage HDD head positioning using an Hinf controller and a tracking differentiator," Mechatronics 19 (2009)

[17] Seung-Hi Lee, et al., "Design of A Dual-stage Actuator Control System with Discrete-Time Sliding Mode for Hard Disk Drives," IEEE Conference on Decision and Control, Australia, December 2000

[18] W.C. Wu, and T.S. Liu, "Sliding mode based learning control for track-following in HDD," Mechatronics 14 (2004)

[19] Tsang-Li Tai, Jian-Shiang Chen, "Discrete-time sliding-mode controller for dual-stage systems -A hierarchical approach," Mechatronics 15 (2005) 949–967

[20] G. Herrmann, et al., "Application of a discrete sliding mode technique to a HDD dual-stage track-seek and track-following servo system," 22nd IEEE International Symposium on Intelligent Control (2007)

[21] Qinglei Hu, et al., "Discrete-Time Sliding Mode Control With Time-Varying Surface for Hard Disk Drives," IEEE Trans Control System Technology, Vol. 17, No. 1, January 2009

[22] Edwards C, Spurgeon SK, Sliding Mode Control: Theory and Applications. Taylor & Francis: U.K., 1998.

[23] Utkin, V. I., Sliding Modes in Control Optimization, Springer-Verlag, Berlin, 1992.

[24] Khalil, H. K., Nonlinear Systems, Prentice Hall, 2001.